CORONAVIRUS

SARS-CoV-2 S2–targeted vaccination elicits broadly neutralizing antibodies

Kevin W. Ng[1]†, Nikhil Faulkner[1,2]†, Katja Finsterbusch[3], Mary Wu[4], Ruth Harvey[5], Saira Hussain[5,6], Maria Greco[6], Yafei Liu[7,8], Svend Kjaer[9], Charles Swanton[10,11,12], Sonia Gandhi[13], Rupert Beale[14], Steve J. Gamblin[15], Peter Cherepanov[16], John McCauley[5], Rodney Daniels[5], Michael Howell[4], Hisashi Arase[7,8,17], Andreas Wack[3], David L.V. Bauer[6], George Kassiotis[1,18]*

Several variants of severe acute respiratory syndrome coronavirus 2 (SARS-CoV-2) have emerged during the current coronavirus disease 2019 (COVID-19) pandemic. Although antibody cross-reactivity with the spike glycoproteins (S) of diverse coronaviruses, including endemic common cold coronaviruses (HCoVs), has been documented, it remains unclear whether such antibody responses, typically targeting the conserved S2 subunit, contribute to protection when induced by infection or through vaccination. Using a mouse model, we found that prior HCoV-OC43 S–targeted immunity primes neutralizing antibody responses to otherwise subimmunogenic SARS-CoV-2 S exposure and promotes S2-targeting antibody responses. Moreover, vaccination with SARS-CoV-2 S2 elicited antibodies in mice that neutralized diverse animal and human alphacoronaviruses and betacoronaviruses in vitro and provided a degree of protection against SARS-CoV-2 challenge in vivo. Last, in mice with a history of SARS-CoV-2 Wuhan–based S vaccination, further S2 vaccination induced broader neutralizing antibody response than booster Wuhan S vaccination, suggesting that it may prevent repertoire focusing caused by repeated homologous vaccination. These data establish the protective value of an S2-targeting vaccine and support the notion that S2 vaccination may better prepare the immune system to respond to the changing nature of the S1 subunit in SARS-CoV-2 variants of concern, as well as to future coronavirus zoonoses.

INTRODUCTION

The ongoing coronavirus disease 2019 (COVID-19) pandemic has highlighted the potential pathogenicity of coronaviruses (CoVs), as well as the gaps in our understanding of immune-mediated protection against this type of infection. The incidence and severity of disease vary widely after infection with severe acute respiratory syndrome CoV 2 (SARS-CoV-2), the etiologic agent of COVID-19, for reasons that remain incompletely understood (1–3). In contrast, four endemic human CoVs (HCoVs) follow a seasonal pattern of circulation and, although they can cause considerable disease in vulnerable populations, they are typically associated with common colds (4, 5).

[1]Retroviral Immunology, The Francis Crick Institute, 1 Midland Road, London NW1 1AT, UK. [2]National Heart and Lung Institute, Imperial College London, London SW3 6LY, UK. [3]Immunoregulation Laboratory, The Francis Crick Institute, 1 Midland Road, London NW1 1AT, UK. [4]High Throughput Screening STP, The Francis Crick Institute, 1 Midland Road, London NW1 1AT, UK. [5]Worldwide Influenza Centre, The Francis Crick Institute, 1 Midland Road, London NW1 1AT, UK. [6]RNA Virus Replication Laboratory, The Francis Crick Institute, 1 Midland Road, London NW1 1AT, UK. [7]Department of Immunochemistry, Research Institute for Microbial Diseases, Osaka University, Osaka 565-0871, Japan. [8]Laboratory of Immunochemistry, World Premier International Immunology Frontier Research Centre, Osaka University, Osaka 565-0871, Japan. [9]Structural Biology STP, The Francis Crick Institute, 1 Midland Road, London NW1 1AT, UK. [10]Cancer Evolution and Genome Instability Laboratory, The Francis Crick Institute, 1 Midland Road, London NW1 1AT, UK. [11]Cancer Research UK Lung Cancer Centre of Excellence, University College London Cancer Institute, London, UK. [12]Cancer Metastasis Laboratory, University College London Cancer Institute, London, UK. [13]Neurodegradation Biology Laboratory, The Francis Crick Institute, 1 Midland Road, London NW1 1AT, UK. [14]Cell Biology of Infection Laboratory, The Francis Crick Institute, 1 Midland Road, London NW1 1AT, UK. [15]Structural Biology of Disease Processes Laboratory, The Francis Crick Institute, 1 Midland Road, London NW1 1AT, UK. [16]Chromatin structure and mobile DNA Laboratory, The Francis Crick Institute, 1 Midland Road, London NW1 1AT, UK. [17]Center for Infectious Disease Education and Research, Osaka University, Osaka 565-0871, Japan. [18]Department of Infectious Disease, St Mary's Hospital, Imperial College London, London W2 1PG, UK.
*Corresponding author. Email: george.kassiotis@crick.ac.uk
†These authors contributed equally to this work.

The initial successes of COVID-19 vaccination campaigns in reducing both the risk of infection with SARS-CoV-2 and the severity of symptoms, even when infection is not prevented, underscore the contribution of adaptive immunity in shaping SARS-CoV-2 pathogenicity. In highly immune populations, SARS-CoV-2 pathogenicity may eventually fall to a degree comparable with that of HCoVs (6). However, the precise nature or targets of a protective immune response to SARS-CoV-2 or CoVs more broadly are only now beginning to emerge (2, 3), with humoral immunity considered the mainstay (7). Yet, despite almost universal seropositivity, HCoVs infect repeatedly (8). Similarly, SARS-CoV-2 reinfections in previously infected individuals and breakthrough SARS-CoV-2 infections in fully vaccinated individuals have been extensively documented (9, 10). These observations indicate that sterilizing immunity to CoVs, at least the type that is induced by infection or current vaccines, is partial and short-lived.

The effectiveness of vaccine-induced immunity to SARS-CoV-2 is further reduced by the emergence of virus variants that are relatively resistant to neutralization by antibodies raised against the spike (S) protein of the earliest SARS-CoV-2 strain isolated in Wuhan, China, which forms the basis of currently licensed vaccines (11–19). Both the SARS-CoV-2 strain carrying the S D614G substitution that quickly replaced the Wuhan strain early during the pandemic and the Alpha strain (B.1.1.7) that arose in the United Kingdom exhibit modest resistance to neutralization by antibodies raised against the Wuhan strain. Other SARS-CoV-2 variants of concern (VOCs), such as Beta (B.1.351), Gamma (B.1.1.28), Delta (B.1.617.2), and, particularly, Omicron (B.1.1.529), exhibit substantially more resistance to neutralization (11–22). Evasion of immunity by VOCs is attributable to amino acid substitutions predominantly in the S1 subunit of the S protein, a subunit that is far less conserved than the S2 subunit. Of all the substitutions in the S proteins of the Alpha, Beta,

Gamma, Delta and Omicron variants, 71 are located in S1, 33 of which are shared among at least two of the variants, and 12 are located in S2, none of which are shared. On the basis of this high number of substitutions in S1, together with their ability to evade antibodies induced by prior S variants, Omicron subvariants may be considered a distinct SARS-CoV-2 serotype (*23*).

As part of full-length S, the S2 subunit harbors a sizeable proportion of epitopes targeted by antibodies in the response to SARS-CoV-2 infection or vaccination (*24–31*). However, despite the higher sequence conservation in S2 among SARS-CoV-2 variants and other CoVs, the antibody repertoire appears to focus on more variable and likely more immunogenic epitopes in the receptor binding domain (RBD) and N-terminal domain of S1 upon repeated infections with homologous and heterologous HCoVs or SARS-CoV-2 strains (*30*, *31*). Nevertheless, cross-reactive antibodies targeting conserved regions in SARS-CoV-2 S2, such as the fusion peptide, heptad repeats (HRs), stem helix, or membrane-proximal regions, have been detected in prepandemic serum samples (*32–35*), likely induced by HCoVs, and are also back-boosted by SARS-CoV-2 infection or vaccination (*16*, *31*, *33*, *35–37*).

Because S2-targeting antibodies do not directly affect binding of the RBD to the main SARS-CoV-2 cellular receptor angiotensin converting enzyme 2 (ACE2), their relative contribution to protection and, by extension, the limits of cross-reactive immunity have been a matter of debate. However, several S2-specific monoclonal antibodies with potent neutralizing activity have been isolated during the previous SARS-CoV pandemic (*38–40*), and more recently during the current SARS-CoV-2 pandemic (*41–46*), implying that broad protection against diverse CoVs may be possible by targeting the S2 subunit (*47*).

Here, we used a mouse model to directly test the contribution of S2-targeting humoral immunity to protection against SARS-CoV-2. We show that prior HCoV-OC43 S immunization primes neutralizing antibody responses to a single SARS-CoV-2 S immunization, which would otherwise be subimmunogenic, and focuses the antibody response to S2. We further show that S2-based vaccination induces robust in vitro neutralization of all human and animal CoVs tested, as well as a degree of in vivo protection against SARS-CoV-2 challenge. Thus, S2 vaccination broadens the antibody response to highly conserved epitopes, forming the basis of a potential pan-CoV vaccine.

RESULTS

Prior HCoV-OC43 S immunity cross-reacts with and primes SARS-CoV-2 S antibody responses

To examine the extent of cross-reactivity between an HCoV S and SARS-CoV-2 S, we immunized C57BL/6J mice with HCoV-OC43 S using two doses of a DNA vaccine administered 4 weeks apart (Fig. 1A). A single dose of the vaccine (prime) did not induce SARS-CoV-2 RBD or S1 cross-reactive immunoglobulin G (IgG) antibodies and only low titers of SARS-CoV-2 S2 cross-reactive IgG antibodies, as detected by enzyme-linked immunosorbent assay (ELISA) (Fig. 1B). The second dose of the vaccine (boost) increased titers of these antibodies, particularly for SARS-CoV-2 S2, which were boosted 2.5 times (Fig. 1B). HCoV-OC43 S immunization also induced neutralizing activity against retroviral vectors pseudotyped with SARS-CoV-2 S, which was, however, one order of magnitude lower than that against homologous HCoV-OC43 S pseudoviruses (Fig. 1C). OC43 S
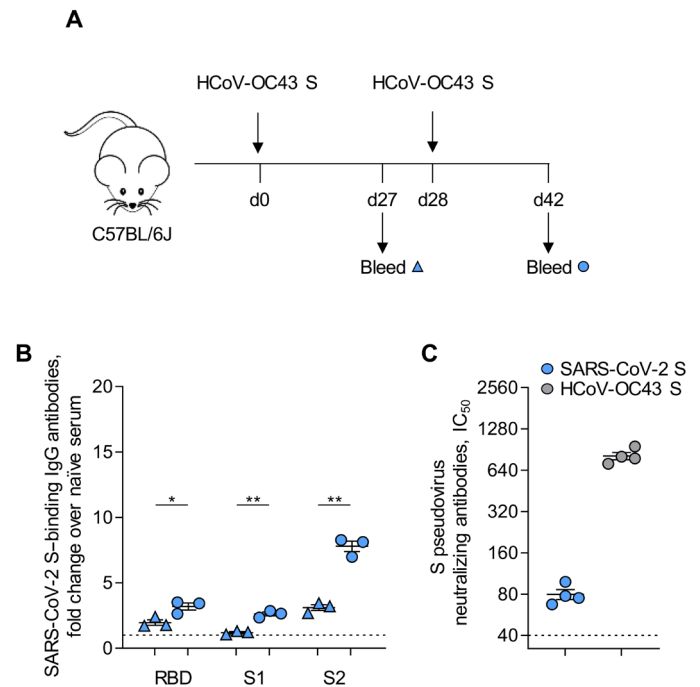

Fig. 1. Prior HCoV-OC43 S immunity cross-reacts with SARS-CoV-2 S. (**A**) A diagram of HCoV-OC43 S immunization regimen and serum sample collection is shown. d, day. (**B**) Titers of ELISA-detected IgG antibodies reacting with SARS-CoV-2 RBD, S1, or S2 were quantified in serum isolated from C57BL/6J mice ($n = 3$) after one or two doses of an HCoV-OC43 S DNA vaccine. The dashed horizontal line indicates the limit of detection. P values were calculated with paired Student's t tests. $*P < 0.05$; $**P < 0.01$. (**C**) Pseudovirus neutralizing antibody titers (IC_{50}) in the serum of mice after two doses of an HCoV-OC43 S DNA vaccine ($n = 4$) were compared with serum from unvaccinated mice ($n = 4$). Neutralization was measured against retroviral vectors pseudotyped with HCoV-OC43 S or SARS-CoV-2 S. The dashed horizontal line indicates the limit of detection. Values in (B) and (C) are from separate experiments and are presented as means ± SEM.

immunization generated antibodies with weak neutralizing activity against authentic SARS-CoV-2 Wuhan and Alpha strains, which was detected by a plaque reduction neutralization test (PRNT) only in some of the mice and only at the highest serum concentration (fig. S1).

Another measure of S cross-reactivity is the ability of one S variant to prime responses to another. To test this, we compared the responses to a single SARS-CoV-2 Wuhan S immunization of C57BL/6J mice that were previously immunized once with HCoV-OC43 S (prime) or not (Fig. 2A). As controls, we used mice immunized twice with either HCoV-OC43 S or SARS-CoV-2 Wuhan S (prime-boost) (Fig. 2A). Again, compared with naïve mice, a single dose of HCoV-OC43 S induced very low titers of SARS-CoV-2 S cross-reactive IgG antibodies (Fig. 2B). As expected, a single dose of SARS-CoV-2 Wuhan S given to previously naïve mice induced ELISA-detectable antibodies that reacted with homologous SARS-CoV-2 RBD, S1, and S2 at comparable titers (Fig. 2B). However, in HCoV-OC43 S–primed mice, a subsequent dose of SARS-CoV-2 Wuhan S induced higher titers specifically of SARS-CoV-2 S2–binding antibodies, which were boosted 1.9 times (Fig. 2B). In contrast, in SARS-CoV-2 S–primed mice, a subsequent dose of SARS-CoV-2 Wuhan S boosted titers of RBD- and S1-reactive IgG antibodies but not those of S2 reactive antibodies (Fig. 2B). Prior HCoV-OC43 S immunization
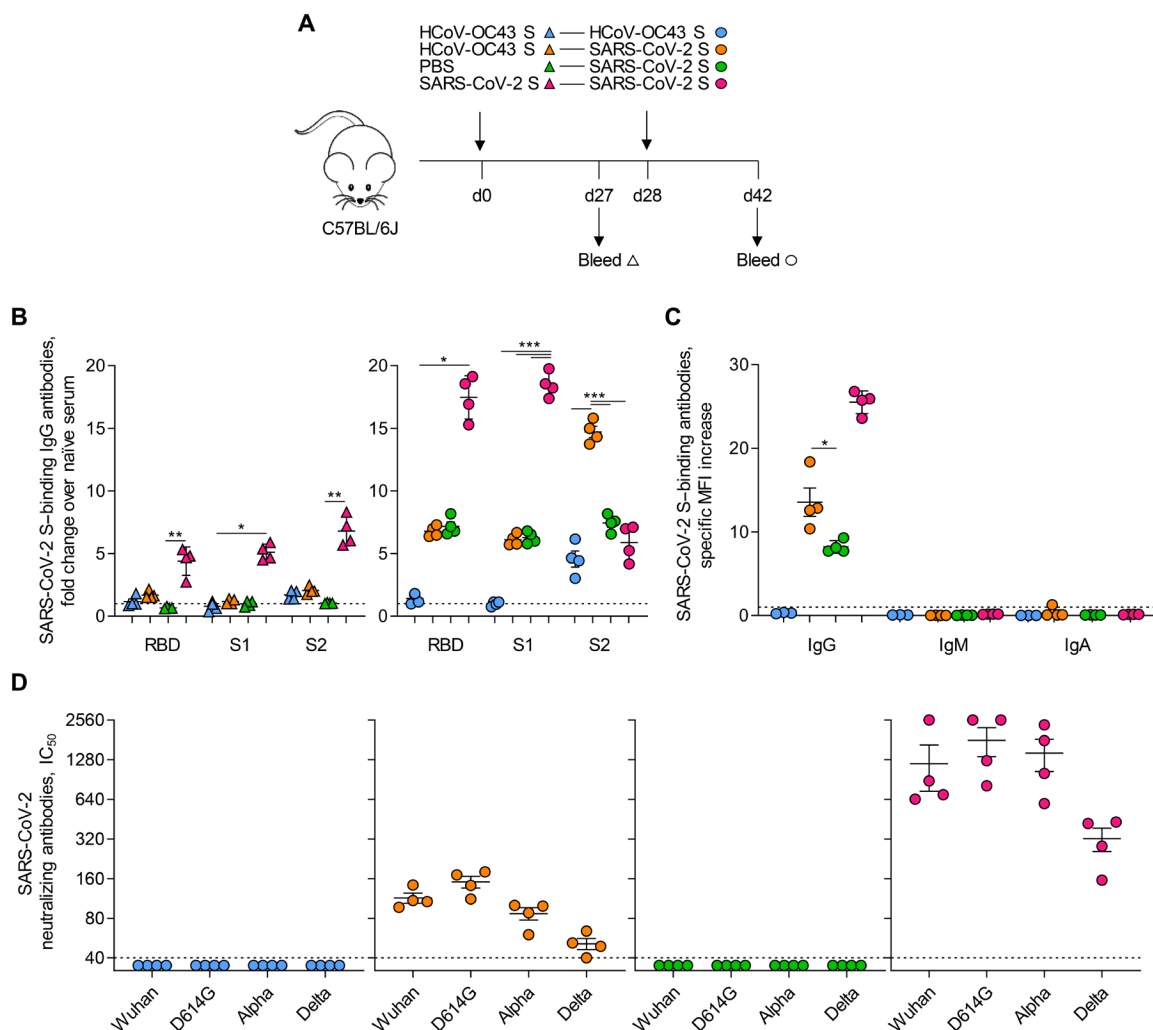
Fig. 2. Prior HCoV-OC43 S immunity primes antibody responses to SARS-CoV-2 S. (**A**) A timeline of HCoV-OC43 S and SARS-CoV-2 immunization regimens and serum sample collections is shown. (**B**) Titers of ELISA-detected IgG antibodies reacting with SARS-CoV-2 RBD, S1, or S2 were determined for serum samples collected from naïve, HCoV-OC43 S–primed, and SARS-CoV-2 S–primed C57BL/6J mice before (left) and after (right) boost with SARS-CoV-2 S ($n = 4$ per group). P values were calculated with ANOVA on ranks tests with Tukey tests or ANOVA tests with Bonferroni t tests for multiple comparisons analysis, respectively. The dashed horizontal line indicates the limit of detection. *$P < 0.05$; **$P < 0.01$; ***$P < 0.001$. (**C**) Titers of IgG, IgM, and IgA antibodies reacting with SARS-CoV-2 S were measured in the serum of mice 2 weeks after the indicated DNA vaccine prime-boost regimen ($n = 4$ for all groups) using a SUP-T1 cell–based assay. P value was calculated with Student's t tests between naïve and HCoV-OC43 S–primed mice both boosted with SARS-CoV-2 S. The dashed horizontal line indicates the limit of detection. *$P < 0.05$. (**D**) Titers (IC_{50}) of antibodies able to neutralize the indicated authentic SARS-CoV-2 strains and VOCs are shown for the same groups of mice in (A) to (C) ($n = 4$ per group). The dashed horizontal line indicates the limit of detection. Data are presented as means ± SEM.

increased titers of IgG antibodies elicited by a single dose of a subsequent SARS-CoV-2 Wuhan S vaccine that bound natural SARS-CoV-2 S conformations in a cell-based assay (Fig. 2C). Moreover, prior HCoV-OC43 S immunization primed production of neutralizing antibodies against authentic SARS-CoV-2 Wuhan and D614G strains, as well as the VOCs tested, detected by a high-throughput World Health Organization (WHO)–benchmarked neutralization assay (Fig. 2D). In contrast, a single dose of the SARS-CoV-2 Wuhan S vaccine induced no measurable neutralizing antibodies against any of the viruses in previously naïve mice (Fig. 2D). Lack of immunogenicity of a single-dose SARS-CoV-2 Wuhan S DNA vaccine in mice differs from observations after a single dose of a SARS-CoV-2 Wuhan S mRNA vaccine in humans, even when then same high-throughput neutralization assay is used (*19*) but is consistent

with reduced overall immunogenicity of DNA vaccines compared with mRNA vaccines (*48*). Together, these results demonstrated that prior HCoV-OC43 S exposure imprinted preferential targeting of the S2 subunit during subsequent SARS-CoV-2 S exposure and enabled the induction of neutralizing antibodies that would not have otherwise been induced by a single SARS-CoV-2 S vaccine dose, thus transforming subimmunogenic SARS-CoV-2 S exposure to immunogenic.

Immunization with membrane-bound SARS-CoV-2 S2 induces broadly neutralizing antibodies

Because HCoV-OC43 S priming enhanced the production both of S2-targeting and of neutralizing antibodies by subsequent SARS-CoV-2 S immunization, we next explored whether the two were

linked. Titers of S2-targeting antibodies could simply reflect titers of RBD-targeting neutralizing antibodies or they could mediate at least part of the increased neutralizing activity. To directly test the ability of S2-targeting antibodies to neutralize SARS-CoV-2 and other CoVs, we immunized C57BL/6J mice with a DNA vaccine encoding the membrane-bound SARS-CoV-2 S2 subunit (24) or with bacterially produced recombinant monomeric SARS-CoV-2 S2 protein, encompassing amino acid residues 686 to 1211 of SARS-CoV-2 Wuhan S. Compared with a DNA vaccine encoding the full-length SARS-CoV-2 S, both the S2 DNA vaccine and the recombinant S2 protein induced more than fourfold higher titers of S2-targeting antibodies as detected by an S2-specific ELISA (Fig. 3A). These results were consistent with preferential targeting of RBD and S1 after repeated immunization with full-length SARS-CoV-2 S (Fig. 2B) and implied that full-length S may stimulate only a fraction of the potential magnitude of the response to S2. However, pertinent to potential neutralization, only antibodies induced by the S2 DNA vaccine, but not by recombinant S2 protein, recognized intact SARS-CoV-2 S in its natural conformation in the cell-based assay (Fig. 3B), suggesting that the S2 construct expressed by the DNA vaccine facilitated preferential targeting of naturally presented epitopes in the full-length S. The inability of recombinant S2 protein to elicit antibodies against the natural conformation of SARS-CoV-2 S was not due to the route of immunization, because the same recombinant S2 protein administered intramuscularly also failed to induce neutralizing antibodies against SARS-CoV-2 Wuhan or Omicron S pseudovirus (fig. S2). In contrast, intramuscular administration of recombinant SARS-CoV-2 Wuhan S1 protein, which was used as a control, induced substantial neutralization of homologous SARS-CoV-2 Wuhan S but not heterologous Omicron S pseudovirus (fig. S2).

The pattern of reactivity with short overlapping peptides in an array covering the SARS-CoV-2 S2 subunit was overall similar between serum from mice immunized with the SARS-CoV-2 S2 DNA vaccine and with recombinant S2 protein, as well as with COVID-19 convalescent human serum samples (fig. S3) (32), and did not reveal major shifts in epitope targeting. Nevertheless, serum from SARS-CoV-2 S2 DNA–vaccinated mice reacted less well with epitopes in the fusion peptide region than with other defined epitopes in S2 and more strongly with an epitope in the membrane-proximal region (fig. S3).

Antibodies induced by SARS-CoV-2 S2 immunization recognized the full-length S not only from the homologous SARS-CoV-2 Wuhan strain but also from all four HCoVs, other SARS-CoV-2 VOCs, and the two bat CoVs, i.e., bat SARS-like CoV WIV1 (Bat SL-CoV-WIV1) and bat CoV RaTG13 (Bat CoV-RaTG13) as tested by flow cytometry in a cell-based assay (Fig. 3C). Furthermore, these antibodies effectively neutralized retroviral vectors pseudotyped with all the CoV S proteins tested (Fig. 3, C and D), including SARS-CoV-2 Omicron S, indicating broad neutralizing ability. In contrast, full-length SARS-CoV-2 Wuhan S vaccination induced antibodies that neutralized vectors pseudotyped with homologous SARS-CoV-2 Wuhan S, but not SARS-CoV-2 Omicron S or the two bat CoV S proteins, and vaccination with recombinant SARS-CoV-2 S2 protein did not induce neutralizing antibodies against any of the pseudoviruses tested (table S1). Moreover, neutralization of SARS-CoV-2 Wuhan or Omicron S pseudoviruses by SARS-CoV-2 S2 DNA vaccine–elicited antibodies was blocked by addition of soluble recombinant SARS-CoV-2 S2, but not RBD (Fig. 3D), indicating that the neutralizing activity was mediated by S2-targeting antibodies. These results

also indicated that putative epitopes of neutralizing S2-targeting antibodies were present in monomeric recombinant S2 protein, although the latter did not induce antibodies that bound the full-length trimeric S on the cell surface or neutralizing antibodies (Fig. 3B and fig. S2).

In the high-throughput authentic virus neutralization assay, antibodies induced by SARS-CoV-2 S2 immunization demonstrated neutralizing activity against SARS-CoV-2 Wuhan and D614G strains, as well as the VOCs tested (Fig. 3E), at titers comparable with those induced by full-length S immunization (Fig. 2D). Relative to recognition of the homologous Wuhan strain, S2 immunization induced neutralizing antibodies that were less sensitive to amino acid substitutions in SARS-CoV-2 S variants than full-length S immunization, as suggested by the difference between the maximally and minimally neutralized SARS-CoV-2 variant, which we consider as an indirect measure of cross-reactivity (Fig. 3F). Therefore, immunization with cell-presented membrane-bound SARS-CoV-2 S2, but not with bacterially produced recombinant S2 protein, induced neutralizing antibodies with broad activity against all animal and HCoVs tested.

Immunization with membrane-bound SARS-CoV-2 S2 affords in vivo protection

Titers of neutralizing antibodies elicited by SARS-CoV-2 S2 immunization were also determined with an authentic virus high-throughput neutralization assay (49), which has been used to establish the WHO International Standard for SARS-CoV-2 antibody neutralization and was benchmarked against this standard (19). The half-maximal inhibitory concentration (IC_{50}) in this assay (18, 19) and in similar assays has been correlated with vaccine efficacy against SARS-CoV-2, including the Delta variant in humans (50–52), suggesting that the neutralizing antibody titers that SARS-CoV-2 S2 immunization induced in mice would also be protective against viral infection in vivo. Nevertheless, to directly test the degree of in vivo protection afforded by SARS-CoV-2 S2 immunization, we next challenged SARS-CoV-2 S2–vaccinated and control unvaccinated mice with SARS-CoV-2 Wuhan or Alpha variants intranasally. Although certain SARS-CoV-2 variants, particularly ones bearing the S N501Y substitution, can replicate in wild-type (WT) C57BL/6J mice using the murine ACE2 as cellular receptor, for this study, we used keratin 18 (K18)–human ACE2 (hACE2) transgenic mice. These mice express hACE2 in epithelial cells under the control of the human K18 promoter (53), which may better capture the ability of antibodies to disrupt virus replication using the human ACE2 receptor. Vaccinated mice were challenged with 3000 plaque-forming units (PFU) of SARS-CoV-2 Wuhan or Alpha strains, a dose that, when given to unvaccinated mice, is sublethal for the homologous SARS-CoV-2 Wuhan strain and lethal for the heterologous Alpha strain (table S2). Given the severe pathology that results from SARS-CoV-2 infection of K18-hACE2 transgenic mice at later time points, infected mice were analyzed 4 days after challenge (Fig. 4A) by expression of the SARS-CoV-2 envelope (E) gene in infected lungs. Compared with unvaccinated controls, SARS-CoV-2 S2–vaccinated mice were considerably more protected against both SARS-CoV-2 Wuhan and Alpha challenge, with 0.9 and 1.1 log reduction in SARS-CoV-2 E copies on day 4, respectively (Fig. 4B and fig. S4), supporting a protective effect of SARS-CoV-2 S2 immunization, as inferred from in vitro neutralization data.
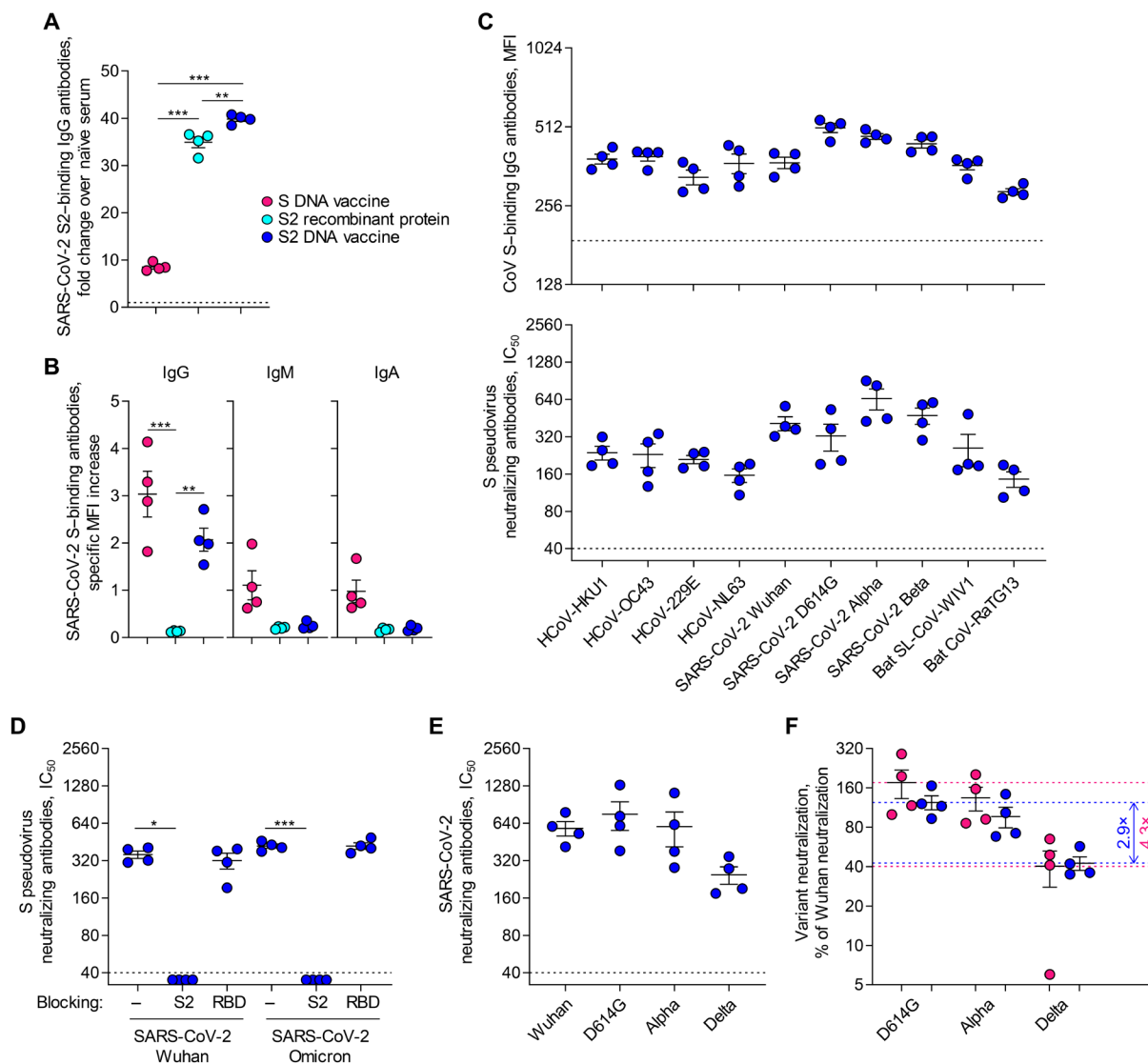
Fig. 3. Immunization with membrane-bound SARS-CoV-2 S2 induces broadly neutralizing antibodies. (**A**) Titers of ELISA-detected IgG antibodies reacting with SARS-CoV-2 S2 were measured in serum samples isolated from C57BL/6J mice (n = 4 per group) after two immunizations with DNA vaccines encoding SARS-CoV-2 full-length S or S2 or with recombinant S2 protein. P values were calculated with ANOVA tests with Bonferroni t tests for multiple comparisons analysis. The dashed horizontal line indicates the limit of detection. **P < 0.01; ***P < 0.001. (**B**) Titers of SARS-CoV-2 full-length S-reactive IgG, IgM, and IgA antibodies in the same serum as in (A) were measured using a SUP-T1 cell–based assay. P values were calculated with ANOVA tests with Bonferroni t tests for multiple comparisons analysis. **P < 0.01; ***P < 0.001. (**C**) Titers of S protein–specific IgG antibodies were quantified in the serum of mice (n = 4 per group) after two immunizations with a SARS-CoV-2 S2 DNA vaccine. Binding titers were measured for S proteins of the indicated human and animal CoVs in the HEK293T cell–based assay (top); corresponding pseudovirus neutralization titers with the same S proteins are also shown (bottom). The dashed horizontal line indicates the limit of detection. (**D**) Antibodies in the serum from the same mice as in (C) were tested for the ability to neutralize retroviral vectors pseudotyped with SARS-CoV-2 Wuhan or Omicron S, in the absence or presence (blocking) of soluble recombinant SARS-CoV-2 Wuhan S2 or RBD. The dashed horizontal line indicates the limit of detection. P values were calculated with ANOVA on ranks with Tukey tests and ANOVA tests with Bonferroni t tests for multiple comparisons analysis for Wuhan and Omicron strains, respectively. *P < 0.05; ***P < 0.001. (**E**) Titers (IC$_{50}$) of antibodies in the same samples as (C) were tested for the ability to neutralize the indicated authentic SARS-CoV-2 strains and VOCs. The dashed horizontal line indicates the limit of detection. (**F**) Neutralization activity was evaluated in serum of mice that received two immunizations with DNA vaccines encoding SARS-CoV-2 full-length S or S2 (n = 4 per group). Neutralization against heterologous SARS-CoV-2 strains and VOCs is expressed as a percentage of neutralization of the homologous Wuhan strain. Data from a single experiment are shown. SARS-CoV-2 S2 immunization was repeated once more with similar results. Dashed horizontal lines mark the average neutralizing activity for the maximally and minimally neutralized groups, and numbers represent the ratio between the two. Data are presented as means ± SEM.

SARS-CoV-2 S2 immunization boosts prior SARS-CoV-2 S–induced cross-reactivity

Repeated immunization with homologous antigens, such as the influenza A vaccine, may boost antibody responses to immunodominant but serotype-specific epitopes, at the expense of less dominant but conserved epitopes, thus progressively narrowing the antibody repertoire and cross-reactivity with heterologous strains (*54*). In standard COVID-19 vaccination campaigns, individuals receive two or
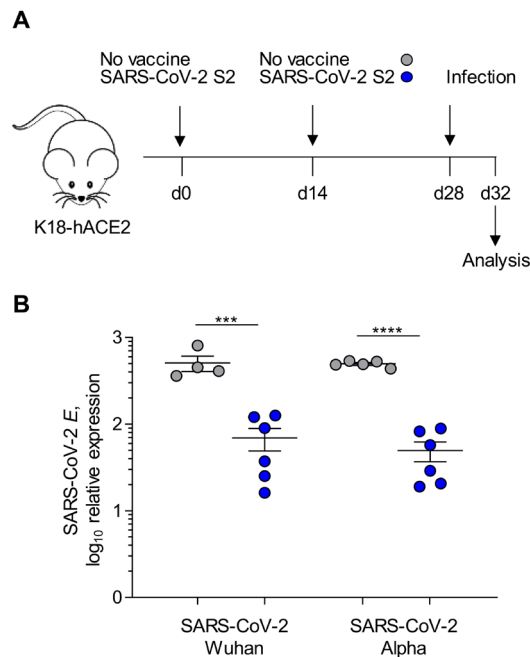
Ng *et al., Sci. Transl. Med.* **14**, eabn3715 (2022)   27 July 2022

5 of 15

Fig. 4. Immunization with membrane-bound SARS-CoV-2 S2 protects against in vivo challenge. (**A**) A timeline of SARS-CoV-2 S2 immunization and SARS-CoV-2 challenge is shown. (**B**) Viral loads were determined by RT-qPCR for SARS-CoV-2 *E* expression in whole lungs from K18-hACE2 transgenic mice that were either un-vaccinated (*n* = 4 to 5) or vaccinated with SARS-CoV-2 S2 DNA vaccine (*n* = 6) and were subsequently challenged with SARS-CoV-2 Wuhan or Alpha. *P* values were calculated with Student's *t* tests. ***$P < 0.001$; ****$P < 0.0001$. Data are presented as means ± SEM.

more doses of a SARS-CoV-2 Wuhan S–based vaccine carrying the same antigen. Although repeated homologous vaccination boosts overall antibody titers, at least transiently, its effect on cross-reactivity with heterologous strains has not yet been established. To mimic at least part of the immunological history imprinted by current vaccination campaigns, we administered two doses of the SARS-CoV-2 Wuhan S vaccine before examining the response to a third dose of either the same vaccine or an S2-targeted vaccine.

A group of C57BL/6J mice were immunized twice with the SARS-CoV-2 Wuhan S DNA vaccine 2 weeks apart and were then split into two groups, each of which received either a third dose of the same vaccine or the SARS-CoV-2 S2 vaccine (Fig. 5A). Two weeks after the third immunization, all serum demonstrated strong neutralization of the immunizing Wuhan strain, as well as the D614G strain and Alpha VOC, which was higher after the S2 vaccine than after the third dose of the full-length S vaccine (Fig. 5B). Differences were more pronounced in neutralization of the Delta VOC, which was generally more resistant to neutralization, with two of six mice in the full-length S vaccine arm lacking detectable titers of Delta neutralizing activity (Fig. 5B). Even when neutralizing antibody titers were normalized to the neutralization of the homologous Wuhan strains, S2 booster immunization elicited more uniform activity against the VOCs tested than full-length S booster immunization, again indicating broader cross-reactivity of the former response (Fig. 5C).

To further compare the neutralization breath of antibodies elicited by either the SARS-CoV-2 Wuhan S or S2 DNA vaccines given as a booster, we tested their neutralizing activity against vectors

pseudotyped with SARS-CoV-2 Omicron S, which exhibits the greatest amino acid sequence divergence among current SARS-CoV-2 VOCs in S1 but retains regions in S2 that are conserved among all CoVs tested (fig. S5). Neutralization of homologous SARS-CoV-2 Wuhan S pseudoviruses by SARS-CoV-2 Wuhan S–elicited serum was sensitive to blocking by the addition of soluble Wuhan RBD but not S2 (Fig. 5D). In contrast, the addition of either soluble Wuhan RBD or S2 reduced, but did not abolish, neutralization of homologous SARS-CoV-2 Wuhan S pseudoviruses by serum isolated from mice vaccinated with the SARS-CoV-2 Wuhan S and S2 combination (Fig. 5E). These observations indicated that repeated SARS-CoV-2 Wuhan S vaccination elicited primarily RBD-targeting neutralizing antibodies, whereas the SARS-CoV-2 Wuhan S and S2 combination regimen elicited neutralizing antibodies targeting both RBD and S2. SARS-CoV-2 Wuhan S–elicited serum failed to neutralize heterologous SARS-CoV-2 Omicron S pseudoviruses (Fig. 5D), in agreement with observations in vaccinated humans (*20–22*). In contrast, serum elicited by the SARS-CoV-2 Wuhan S and S2 combination retained neutralizing activity against SARS-CoV-2 Omicron S pseudoviruses, which was comparable with that against homologous SARS-CoV-2 Wuhan S pseudoviruses and which was mediated by S2-targeting antibodies (Fig. 5E). Together, these results suggested that S2 immunization induces robust immunity against SARS-CoV-2 VOCs even against the backdrop of repeated SARS-CoV-2 full-length Wuhan S immunization.

Last, we examined whether in vitro neutralization of the genetically diverse SARS-CoV-2 strains, such as Omicron (fig. S5), by SARS-CoV-2 Wuhan S2–elicited serum was correlated with survival from a lethal challenge in vivo. However, in vivo challenge with SARS-CoV-2 Omicron failed to induce weight loss or pathological symptoms in unvaccinated K18-hACE2 transgenic mice, even at the highest dose of 50,000 PFU per mouse (table S2), in agreement with recent reports (*55, 56*), and was therefore not used for the challenge of vaccinated mice. Instead, we challenged mice with an equally high dose of the SARS-CoV-2 Delta variant (50,000 PFU). High-dose Delta variant challenge proved lethal for unvaccinated K18-hACE2 transgenic mice, as well as those vaccinated with the SARS-CoV-2 Wuhan S or SARS-CoV-2 Wuhan S and S2 combination regimens (Fig. 5, F and G, and table S2). These results underscore the differential pathogenicity of SARS-CoV-2 Delta and Omicron strains and suggest that neutralizing antibodies elicited by these vaccination regimens can be overwhelmed by a sufficiently high virus inoculum.

DISCUSSION

Mutations acquired by SARS-CoV-2 VOCs that encode certain amino acid substitutions in the S protein reduce the neutralizing ability of antibodies elicited by infection with earlier strains, such as the Wuhan and D614G strains and the Alpha variant (*11–17, 49, 57–60*), as well as of antibodies induced by current COVID-19 vaccines based on the SARS-CoV-2 Wuhan S sequences (*11–19*). The evolution of SARS-CoV-2 S immune evasion warrants consideration of less variable or mutable targets in the S protein and of immunization strategies eliciting broader neutralizing activity. Here, we used a mouse model to test immunity afforded by targeting conserved regions of the S protein; with these data, we provide evidence for a highly protective antibody response targeting the S2 subunit. S2-specific immunity was conferred both by prior exposure to an HCoV, which induced SARS-CoV-2 S2 cross-reactive antibodies,
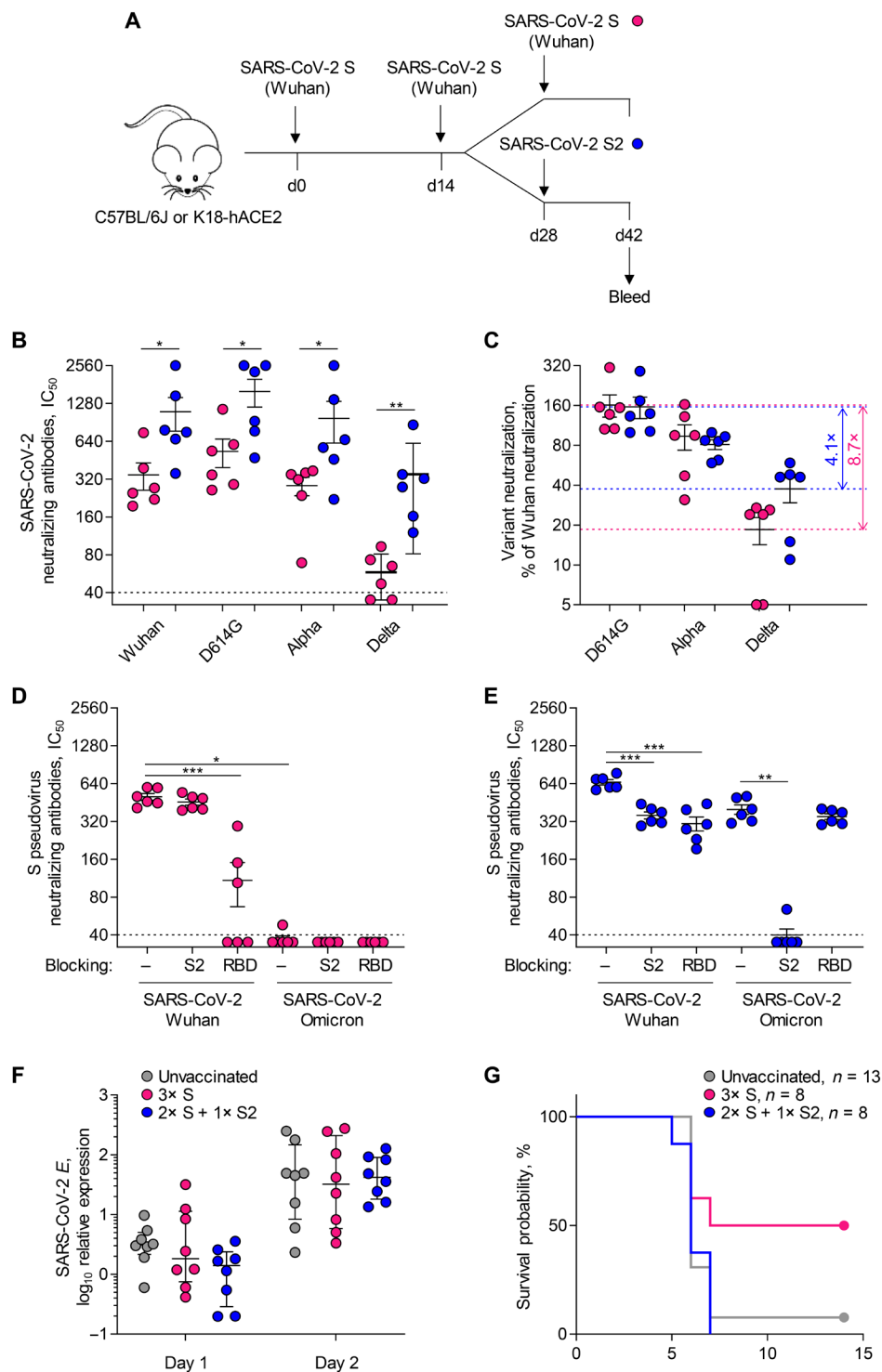
Ng *et al.*, *Sci. Transl. Med.* **14**, eabn3715 (2022)   27 July 2022

6 of 15

Fig. 5. SARS-CoV-2 S2 immunization boosts prior SARS-CoV-2 S–induced cross-reactivity. (**A**) A timeline of SARS-CoV-2 full-length S and S2 immunization regimens and serum sample collection is shown. (**B**) Neutralizing antibody titers (IC_{50}) were quantified in the serum of mice that were immunized twice with SARS-CoV-2 full-length S DNA vaccine and then received a third immunization with either SARS-CoV-2 full-length S or S2 DNA vaccines ($n = 6$ per group). Antibodies were tested for the ability to neutralize the indicated authentic SARS-CoV-2 strains and VOCs. P values were calculated with Student's t tests (D614G) or Mann-Whitney rank sum test (Wuhan, Alpha, and Delta). *$P < 0.05$; **$P < 0.01$. The dashed horizontal line indicates the limit of detection. (**C**) Neutralization activity against heterologous SARS-CoV-2 strains and VOCs in the serum of the same mice is expressed as a percentage of neutralization of the homologous Wuhan strain. Dashed horizontal lines mark the average neutralizing activity for the maximally and minimally neutralized groups, and numbers represent the ratio between the two. (**D**) Pseudovirus neutralizing antibody titers (IC_{50}) were quantified in serum samples from mice ($n = 6$) immunized three times with SARS-CoV-2 full-length S DNA vaccine. Serum was tested for the ability to neutralize retroviral vectors pseudotyped with SARS-CoV-2 Wuhan or Omicron S in the absence or presence (blocking) of soluble recombinant SARS-CoV-2 Wuhan S2 or RBD. P values were calculated with ANOVA tests with Bonferroni t tests for within-variant comparisons and with ANOVA on ranks with Tukey tests for between-variant comparisons. *$P < 0.05$; ***$P < 0.001$. The dashed horizontal line indicates the limit of detection. (**E**) Neutralizing antibody titers (IC_{50}) were measured in serum samples from mice ($n = 6$) immunized twice with SARS-CoV-2 full-length S DNA vaccine and then received a third immunization with SARS-CoV-2 S2 DNA vaccine. Serum samples were tested for the ability to neutralize retroviral vectors pseudotyped with SARS-CoV-2 Wuhan or Omicron S, in the absence or presence (blocking) of soluble recombinant SARS-CoV-2 Wuhan S2 or RBD. P values were calculated with ANOVA test with Bonferroni t test for within-Wuhan comparisons and with ANOVA on ranks with Tukey tests for within-Omicron and between-variant comparisons. **$P < 0.01$; ***$P < 0.001$. The dashed horizontal line indicates the limit of detection. (**F**) Viral loads, determined by RT-qPCR for SARS-CoV-2 E expression, were quantified in nasal swabs from K18-hACE2 transgenic mice that were either unvaccinated ($n = 8$), vaccinated three times with SARS-CoV-2 S DNA vaccine (3× S, $n = 8$), or vaccinated twice with the SARS-CoV-2 S DNA vaccine and once with the SARS-CoV-2 S2 DNA vaccine (2× S + 1× S2, $n = 8$), as in (A), and were subsequently challenged with SARS-CoV-2 Delta. (**G**) Survival probabilities, calculated by a 25% weight loss end point, for the same groups as in (F). Survival distributions were compared by a log-rank test, and differences were not statistically significant. Data in (B) to (F) are presented as means ± SEM.

and by deliberate immunization with a SARS-CoV-2 S2–encoding DNA vaccine.

Although induction of S2-targeting cross-reactive antibodies by HCoV or SARS-CoV-2 infection or COVID-19 vaccination is now well recognized (16, 31–37, 41, 43–46), their potential contribution to the outcome or severity of SARS-CoV-2 infection remains to be established (47). A potential protective effect mediated by such antibodies is suggested by certain studies linking an early S2-targeted antibody response to SARS-CoV-2 with milder symptoms and survival of COVID-19 (61–66). However, detrimental effects of cross-reactive or preexisting immunity, such as original antigenic sin, have also been hypothesized, although not always directly attributed to S2-targeting antibodies (24, 67–69).

Our observation that prior exposure of immunologically naïve mice to HCoV-OC43 S promotes S2-targeting cross-reactive antibodies and primes for induction of SARS-CoV-2 neutralizing antibodies that would not have otherwise been elicited after a single SARS-CoV-2 immunization provides direct evidence for a cross-protective effect. No evidence consistent with original antigenic sin was obtained in this model. In contrast, Lapp et al. (70) observed that priming of mice with HCoV-HKU1 induced SARS-CoV-2 S cross-reactive antibodies but impeded the neutralizing antibody response to subsequent SARS-CoV-2 immunization. However, in contrast to the mouse experiment, they also found that preexisting HCoV-HKU1 antibodies correlated positively with SARS-CoV-2 neutralizing antibodies in children after natural infection (70). Although it is theoretically possible that different HCoVs either impede or promote a subsequent antibody response to SARS-CoV-2, an alternative explanation resides in the fact that Lapp et al. (70) used recombinant proteins for immunization of mice. In contrast to immunization with RNA or DNA vectors or natural infection, both of which produce the natural S conformations presented on the surface of cells or virions, recombinant protein immunization may not effectively prime neutralizing antibodies. Immunization with recombinant SARS-CoV-2 S2 in this study induced high titers of antibodies able to bind recombinant S2 on ELISA but unable to bind the full-length S protein presented on cells. In support of this notion, nearly one in three antibodies cloned from a SARS-CoV convalescent donor that cross-reacted with SARS-CoV-2 S recognized the full-length S expressed on the surface of cells but not recombinant S ectodomain (71).

Contrasting with recombinant S2 protein, the SARS-CoV-2 S2–encoding vaccine used here induced a highly protective and broadly neutralizing response. Eliciting protective antibodies against the S2 subunit has been attempted already during the SARS-CoV epidemic in 2005, but not always successfully. Guo et al. (72) reported that immunization of mice with either a recombinant SARS-CoV S2 fragment or a DNA vaccine encoding SARS-CoV S2 induced high titers of S2-binding antibodies but no SARS-CoV neutralizing activity. Using a smaller recombinant SARS-CoV S2 fragment, encompassing the connector domain, stem helix, HR2, and membrane-proximal regions (corresponding to $S_{1073-1210}$ of SARS-CoV-2 S), Keng et al. (73) elicited strong neutralizing activity against SARS-CoV in immunized rabbits and isolated neutralizing monoclonal antibodies targeting separate epitopes in the stem helix, HR2, and membrane-proximal regions in a follow-up study (38). More recently, Ma et al. (74) reported that mice immunized with a combination of nanoparticle vaccines displaying either SARS-CoV-2 RBD or an SARS-CoV-2 S2 fragment from HR1 to HR2 ($S_{910-1213}$), but not those immunized

with SARS-CoV-2 RBD alone, elicited neutralizing antibodies against SARS-CoV, MERS-CoV (Middle East respiratory syndrome CoV), HCoV-229E, HCoV-OC43, and Bat CoV-RaTG13 S pseudoviruses. Although nanoparticles displaying the SARS-CoV-2 S2 fragment were not tested in isolation in this study, the findings do suggest that the observed broad neutralization was likely mediated by S2-targeting antibodies (74).

The isolation of highly neutralizing S2 cross-reactive monoclonal antibodies demonstrates the potential for broad and effective targeting of conserved epitopes on S2. Several monoclonal antibodies targeting the stem helix or base of S2 have now been reported to neutralize several betacoronaviruses, but not human alphacoronaviruses, where this region of S2 is less conserved (41, 43–45, 75). An antibody targeting the more conserved hinge region ($S_{980-1006}$) of S2, however, is reported to neutralize both alphacoronaviruses and betacoronaviruses (46). Despite the presence of cross-reactive epitopes, monoclonal antibodies reactive to the fusion peptide region have not been reported to date. Nevertheless, vaccination of pigs with SARS-CoV-2 fusion peptide expressed on the surface of bacteria induced protective immunity against the porcine epidemic diarrhea virus, an animal CoV sharing sequence similarity in its S2 subunit with that of SARS-CoV-2 and other CoVs (76).

Note that, to the extent indicated by the use of short overlapping peptides here, serum from S2-immunized mice appears to target the hinge region and central helix more strongly than the fusion peptide or the stem helix. These regions are considerably more conserved among human and animal CoVs than other regions of S2, and S2 as a whole is far more conserved than S1. Although amino acid substitutions in S2 are rarer than in S1, they may still have importance (27). For example, the D796H substitution in the highly conserved S_{796} position of S2 upstream of the fusion peptide has been selected for its ability to evade serum neutralization as a result of immune serum therapy for an immunodeficient patient with COVID-19 (77); this mutation is also found in the B.1.1.318 lineage (78). Resistance to neutralization and viral rebound conferred by the D796H substitution is consistent with a prominent role for S2-targeting antibodies in the control of SARS-CoV-2, but it also incurs substantial fitness cost (77). Therefore, although possible, evasion of humoral immunity may be more difficult to achieve by amino acid substitutions in critical regions of S2 without loss of virus fitness. Independently of the precise epitopes targeted in these mice, our data provide evidence that S2-based immunization can induce broad in vitro neutralization of diverse alphacoronaviruses and betacoronaviruses, including human and animal CoVs. S2 immunization may also render mice resistant to in vivo challenge with SARS-CoV-2, linking in vitro neutralization and in vivo protection.

However, our study has several limitations. First, we elicited antibodies in mice only through DNA vaccination, whereas other vaccination regimens, such as RNA vaccines, may be more immunogenic (48). Second, immune priming and boosting were restricted to the S proteins of HCoV-OC43 and SARS-CoV-2 Wuhan strains, whereas the immunological history of humans is likely to be far more complex, involving repeated prior exposure to additional HCoVs and SARS-CoV-2 infection and vaccination. Third, we have only demonstrated in vivo protection elicited by SARS-CoV-2 Wuhan S2 vaccination against SARS-CoV-2 Wuhan and Alpha strains, but we were unable to test protection against more recent VOCs, such as Delta and Omicron, owing to their excessive and reduced pathogenicity,

respectively. Last, we have studied in vitro neutralization of diverse animal and HCoVs as a surrogate for in vivo protection, but the latter may also use additional, neutralization-independent functions of the elicited antibodies, such as Fc-dependent antibody activity, which may contribute substantially to in vivo protection, particularly by S2-targeting cross-reactive antibodies (66).

The data presented here argue that S2 targeting may be an important component of a pan-CoV vaccine. Alternative approaches based on mosaic, combination, or multimeric nanoparticles (79–81) displaying RBDs from diverse CoVs, SARS-CoV-2 S-ferritin nanoparticles (82, 83), or mRNA vaccines encoding chimeric S proteins (84) have all elicited potent broadly neutralizing activity against relevant human and animal CoVs. However, this activity was restricted primarily to the *Sarbecovirus* subgenus of betacoronaviruses and did not extend to alphacoronaviruses. Although it is unlikely that any CoV vaccine will induce full, life-long immunity, our findings suggest that the antibody repertoire could be primed or periodically reset to focus on more conserved regions in S2. This could be achieved using multivalent vaccines combining full-length S proteins of two or three most relevant SARS-CoV-2 VOCs with SARS-CoV-2 S2, at a ratio that ensures a balanced response to diverse S1 and conserved S2 epitopes. Once a protective degree of S2-targeting immunological memory is established, then repeated natural exposure to endemic HCoVs or to an endemic attenuated SARS-CoV-2 variant could be leveraged to maintain cross-reactive responses to current or future pandemic-causing CoVs.

MATERIALS AND METHODS

Study design
This study was designed to assess the therapeutic potential of targeted CoV S2 vaccination against SARS-CoV-2 and other human and animal CoVs. We tested nucleic acid– and protein-based vaccine candidates targeting SARS-CoV-2 S and its constituent subunits using a prime-boost system in WT or K18-hACE2 transgenic mice and tested in vitro activity of serum antibodies and in vivo protection after SARS-CoV-2 challenge. Sample sizes for all animal experiments were estimated on the basis of prior experience to provide statistical power while minimizing animal use and were not altered over the course of the study. Time points were defined on the basis of prior experience and were not altered over the course of the study, and mice were randomly assigned to treatment groups before the start of each experiment. Antibody binding against CoV S proteins and their subunits was assessed by ELISA against SARS-CoV-2 S subunits and flow cytometry on cells transfected with expression vectors encoding S from HCoVs, SARS-CoV-2 (including variants), and bat CoVs. In vitro neutralization titers were determined using green fluorescent protein (GFP)–expressing retroviruses pseudotyped with various CoV S proteins, as well as two separate neutralization assays using authentic SARS-CoV-2 viruses. For all in vitro analyses, at least two technical replicates were performed per biological replicate, and the data represent the average of the technical replicates. Investigators performing live virus neutralization and in vivo infection were blinded until after the experiment and analysis were completed. No samples were excluded from analysis.

Mice
WT C57BL/6J and K18-hACE2 transgenic mice (53) on a C57BL/6J background were obtained from The Jackson Laboratory. Mice were bred and maintained at the Biological Research Facility of The Francis Crick Institute under specific pathogen–free conditions. All experiments were approved by the ethical committee of The Francis Crick Institute and conducted according to local guidelines and U.K. Home Office regulations under the Animals Scientific Procedures Act 1986 (project license numbers PCD77C6D0 and P9C468066).

Virus isolates
SARS-CoV-2 virus isolates were obtained and propagated as previously described (19, 32, 49, 59). The SARS-CoV-2 reference isolate (Wuhan) was hCoV-19/England/02/2020 obtained from Public Health England (PHE). The D614G strain (B.1.1) was isolated from a swab from an infected health care worker at University College London Hospital, obtained through the SAFER (SARS-CoV-2 Acquisition in Frontline Health Care Workers–Evaluation to Inform Response) study (85) and carries only the D614G substitution in S (19). The Alpha (B.1.1.7) isolate was hCoV-19/England/204690005/2020, carrying the D614G, Δ69–70, Δ144, N501Y, A570D, P681H, T716I, S982A, and D1118H substitutions in S, and was obtained from PHE, through W. Barclay, Imperial College London, and G2P-UK (Genotype-to-Phenotype UK) National Virology Consortium. The Delta isolate (B.1.617.2) was MS066352H (GISAID EpiCov accession number EPI_ISL_1731019), carrying the T19R, K77R, G142D, Δ156–157/R158G, A222V, L452R, T478K, D614G, P681R, and D950N substitutions in S, and was provided by W. Barclay, Imperial College London, through G2P-UK. The Omicron (BA.1) isolate was M21021166, carrying the A67V, Δ69–70, T95I, Δ142–144, Y145D, Δ211, L212I, G339D, S371L, S373P, S375F, K417N, N440K, G446S, S477N, T478K, E484A, Q493R, G496S, Q498R, N501Y, Y505H, T547K, D614G, H655Y, N679K, P681H, A701V, N764K, D796Y, N856K, Q954H, N969K, and L981F substitutions in S, and was provided by G. Screaton, University of Oxford, through G2P-UK. All viral isolates were propagated in Vero V1 cells.

Immunizations and infections
For protein immunization, mice were injected intraperitoneally with 25-μg recombinant SARS-CoV-2 S2 (CV2006, LifeSensors) in monophosphoryl lipid A adjuvant (Sigma Adjuvant System, Sigma-Aldrich) in a 100-μl volume. This SARS-CoV-2 S2 protein encompasses amino acid residues 686 to 1211 of SARS-CoV-2 Wuhan S (UniProt ID: P0DTC2), tagged by a His6-SUMO tag, and was produced recombinantly in *Escherichia coli* (CV2006, LifeSensors). For DNA immunization, mice were injected intravenously or intramuscularly with 100 μl of plasmid DNA (1.6 mg/ml) complexed with 1.21 mM GL67 lipid (Genzyme). Serum was collected by venipuncture or terminal bleed into serum separator tubes, centrifuged at 3000 rpm for 5 min after 30 min to allow for clotting, and then centrifuged at 12,000 rpm for 5 min. Serum was then heat-inactivated at 56°C for 10 min and stored at −20°C. For in vivo challenge, naïve or immunized K18-hACE2 transgenic mice were infected intranasally with 3000 PFU of SARS-CoV-2 Wuhan or Alpha strains or 50,000 PFU of SARS-CoV-2 Delta or Omicron strains in 50 μl of phosphate-buffered saline (PBS) under light anesthesia (3% isoflurane) in biosafety containment level 4 facilities. Preinfection body weights were recorded, and mice were weighed daily and monitored for clinical symptoms.

Cell lines and plasmids
Human embryonic kidney (HEK) 293T, Vero E1, Vero E6, and SUP-T1 cells were obtained from the Cell Services facility of The

Francis Crick Institute and verified as mycoplasma-free. All human cell lines were further validated by DNA fingerprinting. Cells were grown in Iscove's modified Dulbecco's medium (Sigma-Aldrich) with 5% fetal bovine serum (Thermo Fisher Scientific), 2 mM L-glutamine (Thermo Fisher Scientific), penicillin (100 U/ml) (Thermo Fisher Scientific), and streptomycin (0.1 mg/ml) (Thermo Fisher Scientific). HEK293T cells expressing CoV S proteins were generated by transient transfection using pcDNA3- or pCMV3-based expression plasmids and GeneJuice (EMD Millipore) 48 hours before use, as previously described (fig. S6) (32, 49, 86). The expression vector (pME18S) encoding SARS-CoV-2 S2 was described previously (24). Briefly, it combines a signal sequence and transmembrane domain from signaling lymphocytic activation molecule and paired Ig-like type 2 receptor α proteins respectively (87) with SARS-CoV-2 $S_{588-1219}$, which covers the last 97 amino acid residues of S1 and the whole S2 ectodomain (24). Expression vectors (pcDNA3) carrying a codon-optimized gene encoding the WT or D614G SARS-CoV-2 S (UniProt ID: P0DTC2) were provided by M. Pizzato, University of Trento. Expression vectors (pcDNA3) carrying codon-optimized genes encoding the Alpha, Beta, or Omicron BA.1 SARS-CoV-2 S variants (49), or Bat SL-CoV-WIV1 (UniProt ID: U5WI05) or Bat CoV-RaTG13 (UniProt ID: A0A6B9WHD3) S proteins were generated in-house. Expression vectors (pCMV3) encoding HCoV-229E S (UniProt ID: APT69883.1), HCoV-NL63 S (UniProt ID: APF29071.1), HCoV-OC43 S (UniProt ID: AVR40344.1), or HCoV-HKU1 S (UniProt ID: Q0ZME7.1) were obtained from SinoBiological. SUP-T1 cells stably expressing SARS-CoV-2 S protein and GFP were generated as described previously (86).

Flow cytometric detection of antibodies

Serum antibodies against CoV S proteins were quantified as described previously (32, 86). Briefly, HEK293T cells were transfected to express various S proteins 48 hours before use, trypsinized, and dispensed into V-bottom 96-well plates (20,000 to 40,000 cells per well). S^+GFP^+ SUP-T1 cells were mixed 1:1 with parental GFP^- SUP-T1 cells before dispensing into V-bottom 96-well plates (20,000 to 40,000 total cells per well) (86). Cells were incubated with serum (diluted 1:50 in PBS) for 30 min and then washed with fluorescence-activated cell sorting (FACS) buffer consisting of PBS, 5% bovine serum albumin (BSA), and 0.05% sodium azide. Samples were then stained with fluorescein isothiocyanate–conjugated anti-mouse IgG (Poly4053, BioLegend), allophycocyanin-conjugated IgA (Clone 11-44-2, Southern Biotech), and phycoerythrin-conjugated IgM (Clone RMM-1, BioLegend) diluted 1:200 in FACS buffer for 30 min. Cells were washed with FACS buffer and analyzed on a Ze5 analyzer (Bio-Rad) running Bio-Rad Everest software v2.4 and analyzed using FlowJo v10 (Tree Star Inc.). For SUP-T1 cells, specific mean fluorescence intensity (MFI) increase caused by immune serum (fig. S7) was calculated using the following formula: (MFI of S^+ SUP-T1 − MFI of parental SUP-T1)/MFI of parental SUP-T1.

ELISA detection of antibodies

ELISAs were run as previously described (32, 86) using in-house recombinant SARS-CoV-2 S1 and RBD and commercial S2 (CV2006. Life Sensors). After incubation with serum (diluted 1:50 in PBS), plates were washed and incubated with horseradish peroxidase (HRP)–conjugated anti-mouse IgG (ab6728, Abcam). Plates were developed by adding 50 µl of 3,3′,5,5′-tetramethylbenzidine (TMB)

substrate for 5 min with shaking (Thermo Fisher Scientific), followed by 50 µl of TMB stop solution (Thermo Fisher Scientific). Optical densities were measured at 450 nm on a Tecan microplate reader, and results were expressed as fold change of optical densities between samples and naïve serum controls.

Pseudotyped virus neutralization

Lentiviral particles were pseudotyped with CoV S proteins as previously described (32). Briefly, HEK293T cells were transfected using GeneJuice (EMD Millipore) with plasmids encoding CoV S proteins, SIVmac Gag-Pol, and HIV-2 backbone encoding GFP. Virus-containing supernatants were collected 48 hours after transfection and stored at −80°C until further use. For neutralization assays, pseudotyped viruses were incubated with serial dilutions of serum at 37°C for 30 min and added to Vero E6 cells seeded in 96-well plates (3000 cells per well). Pseudotyped virus preparations were titrated in Vero E6 cells and were used at a dose that resulted in 1.5 to 10% transduction efficiency (GFP^+ cells) in the absence of serum. Polybrene (4 µg/ml; Sigma-Aldrich) was added to the cells, which were then spun at 1200 rpm for 45 min. GFP^+ cells were quantified by flow cytometry 72 hours after transduction (fig. S8), and the inverse serum dilution leading to a 50% reduction in GFP^+ cells was taken as the neutralizing titer. In some experiments, neutralization was blocked by the addition of soluble recombinant SARS-CoV-2 Wuhan RBD (in-house) or S2 (10 µg/ml) (CV2006; Life Sensors), during incubation of serum and pseudotyped virus.

Authentic virus neutralization

SARS-CoV-2 neutralizing antibody titers were determined using PRNT and high-throughput immunofluorescence assays, as previously described (19, 32, 49). For PRNT assays, triplicate cultures of Vero E6 cells were incubated with 10 to 20 PFU of SARS-CoV-2 variants and serial dilutions of heat-inactivated serum for 3 hours, and the inoculum was removed and overlaid with virus growth medium containing 1.2% Avicel (FMC BioPolymer). Twenty-four hours later, cells were fixed in 4% paraformaldehyde and permeabilized with 0.2% Triton X-100 in PBS. Virus plaques were visualized by immunostaining with a rabbit polyclonal anti-NSP8 antibody (ABIN233792, Antibodies Online) and an HRP-conjugated anti-rabbit antibody (1706515, Bio-Rad), both used at 1:1000 dilution. Plaques were quantified and IC_{50} values calculated using LabView or SigmaPlot software as previously described (32). For high-throughput immunofluorescence assays, Vero E6 cells were seeded in 384-well plates and, at 90 to 100% confluency, were infected with SARS-CoV-2 variants at a multiplicity of infection of about 1 in the presence of serial dilutions of heat-inactivated serum or synthetic monoclonal antibodies. Plates were incubated for a further 24 hours, fixed in 4% paraformaldehyde, blocked, and permeabilized with 3% BSA and 0.2% Triton X-100 in PBS. Cells were immunostained with 4′,6-diamidino-2-phenylindole (DAPI) and Alexa Fluor 488–conjugated anti-nucleocapsid (N) antibody (CR3009, produced in-house) and imaged using an Opera Phenix (PerkinElmer). The ratio of infected (Alexa Fluor 488$^+$) to total cellular (DAPI$^+$) area per well was determined using Harmony (PerkinElmer) and IC_{50} values calculated as previously described (49). Performance of this high-throughput neutralization assay has been benchmarked across laboratories participating in the establishment and validation of the WHO International Standard for SARS-CoV-2 antibody neutralization (WHO/BS.2020.2403) (19).

RNA isolation and reverse transcription quantitative polymerase chain reaction

Mouse lungs were harvested, placed in RNAlater (Ambion), and stored at −80°C. The lungs were homogenized with a FastPrep-24 5G instrument using TallPrep Lysing Matrix M tubes (catalog no. 116949025, MP Biomedicals) in 2 ml of TRIzol, and RNA was isolated using the RiboPure Kit (catalog no. AM1924, Invitrogen) according to the manufacturer's instructions. Five hundred nanograms of RNA was reverse-transcribed using the qPCRBIO complementary DNA (cDNA) synthesis kit according to the manufacturer's instructions. Nasal swabs were collected with prewetted swabs in 350 µl of RLT lysis buffer supplemented with β-mercaptoethanol. RNA was extracted using the RNeasy Micro Kit (Qiagen, 74106) according to the manufacturer's instructions. Provided poly-A RNA was used as carrier RNA to improve the recovery of total RNA. cDNA was generated using the qPCRBIO cDNA synthesis kit (PCRBiosystem; PB30.11-10) as per manufacturer's instructions. Reverse transcription quantitative polymerase chain reaction (RT-qPCR) was performed on an Applied Biosystems QuantStudio 3 machine using the following TaqMan primers for *Hprt1* (Mm00446968_m1): forward: 5′-ACAGGTACG TTAATAGTTAATAGAGCGT-3′; reverse: 5′-ATATTGCAGCAG-TACGCACACA-3′; and probe: FAM-5'-ACACTAGCCATCCT-TACTGCGCTTCG-3′-TAMRA. TaqMan primers for SARS-CoV-2 *E* gene were as previously described (*88*). SARS-CoV-2 *E* values were normalized to the housekeeping gene *Hprt1*. A standard curve of SARS-CoV-2 *E* gene copies was generated by titrating the amount of plasmid DNA of a retrovirus vector (pRV) carrying the SARS-CoV-2 *E* gene (generated in-house) to correspond to 1.5 to 1.5×10^8 copies per reaction.

Peptide array

Antibody reactivity with a peptide array (12-mers overlapping by 10 amino acid residues) spanning the last 743 amino acids of SARS-CoV-2 S was carried out as previously described (*32*), except serum from immunized mice was used as the primary antibody and IRDye 800CW Goat anti-mouse IgG (1:15,000 in blocking buffer; LI-COR) was used as a secondary antibody. Membranes were imaged on an Odyssey CLx Infrared scanner (LI-COR). Scanned images were analyzed in Image Studio v5.2 (LI-COR).

Sequence alignment

Alignment of the amino acid sequences of S proteins of SARS-CoV-2 strains Wuhan, D614G, Alpha, Beta, Delta, and Omicron; the four HCoVs HCoV-229E, HCoV-NL63, HCoV-OC43, and HCoV-HKU1; and two bat CoVs Bat SL-CoV-WIV1 and Bat CoV-RaTG13 was performed using the AlignX component of Vector NTI v11.5. A guide tree, akin to a phylogenetic tree, was built using the neighbor-joining method. This method calculates a matrix of distances between all pairs of sequence analyzed.

Statistical analyses

Raw, individual-level data for experiments where *n* < 20 are presented in data file S1. Data were analyzed and plotted in GraphPad Prism v8 (GraphPad Software) or SigmaPlot v14.0 (Systat Software). Parametric comparisons of normally distributed values that satisfied variance criteria were made using paired or unpaired Student's *t* tests (two groups) or one-way analysis of variance (ANOVA) tests (three or more groups). Data that did not pass the variance criteria were compared using nonparametric two-tailed Mann-Whitney

rank sum tests (two groups) or ANOVA on ranks tests (three or more groups). Multiple comparisons analysis of ANOVA and ANOVA on ranks test results were carried out using the Bonferroni *t* test and Tukey test, respectively. Survival distributions were compared with a log-rank test. Results were considered significant at *$P \leq 0.05$, **$P \leq 0.01$, ***$P \leq 0.001$, and ****$P \leq 0.0001$.

SUPPLEMENTARY MATERIALS

www.science.org/doi/10.1126/scitranslmed.abn3715
Figs. S1 to S8
Tables S1 and S2
MDAR Reproducibility Checklist
Data file S1
View/request a protocol for this paper from *Bio-protocol*.

REFERENCES AND NOTES

1. B. Hu, H. Guo, P. Zhou, Z.-L. Shi, Characteristics of SARS-CoV-2 and COVID-19. *Nat. Rev. Microbiol.* **19**, 141–154 (2020).
2. T. Carvalho, F. Krammer, A. Iwasaki, The first 12 months of COVID-19: A timeline of immunological insights. *Nat. Rev. Immunol.* **21**, 245–256 (2021).
3. A. Sette, S. Crotty, Adaptive immunity to SARS-CoV-2 and COVID-19. *Cell* **184**, 861–880 (2021).
4. R. W. Aldridge, D. Lewer, S. Beale, A. M. Johnson, M. Zambon, A. C. Hayward, E. B. Fragaszy, Seasonality and immunity to laboratory-confirmed seasonal coronaviruses (HCoV-NL63, HCoV-OC43, and HCoV-229E): Results from the Flu Watch cohort study. *Wellcome Open Res.* **5**, 52 (2020).
5. R. Dijkman, M. F. Jebbink, E. Gaunt, J. W. Rossen, K. E. Templeton, T. W. Kuijpers, L. van der Hoek, The dominance of human coronavirus OC43 and NL63 infections in infants. *J. Clin. Virol.* **53**, 135–139 (2012).
6. S. M. Kissler, C. Tedijanto, E. Goldstein, Y. H. Grad, M. Lipsitch, Projecting the transmission dynamics of SARS-CoV-2 through the postpandemic period. *Science* **368**, 860–868 (2020).
7. T. Zohar, G. Alter, Dissecting antibody-mediated protection against SARS-CoV-2. *Nat. Rev. Immunol.* **20**, 392–394 (2020).
8. A. W. D. Edridge, J. Kaczorowska, A. C. R. Hoste, M. Bakker, M. Klein, K. Loens, M. F. Jebbink, A. Matser, C. M. Kinsella, P. Rueda, M. Ieven, H. Goossens, M. Prins, P. Sastre, M. Deijs, L. van der Hoek, Seasonal coronavirus protective immunity is short-lasting. *Nat. Med.* **26**, 1691–1693 (2020).
9. V. J. Hall, S. Foulkes, A. Charlett, A. Atti, E. J. M. Monk, R. Simmons, E. Wellington, M. J. Cole, A. Saei, B. Oguti, K. Munro, S. Wallace, P. D. Kirwan, M. Shrotri, A. Vusirikala, S. Rokadiya, M. Kall, M. Zambon, M. Ramsay, T. Brooks, C. S. Brown, M. A. Chand, S. Hopkins, SARS-CoV-2 infection rates of antibody-positive compared with antibody-negative health-care workers in England: A large, multicentre, prospective cohort study (SIREN). *Lancet* **397**, 1459–1469 (2021).
10. M. Bergwerk, T. Gonen, Y. Lustig, S. Amit, M. Lipsitch, C. Cohen, M. Mandelboim, E. G. Levin, C. Rubin, V. Indenbaum, I. Tal, M. Zavitan, N. Zuckerman, A. Bar-Chaim, Y. Kreiss, G. Regev-Yochay, Covid-19 breakthrough infections in vaccinated health care workers. *N. Engl. J. Med.* **385**, 1474–1484 (2021).
11. V. V. Edara, C. Norwood, K. Floyd, L. Lai, M. E. Davis-Gardner, W. H. Hudson, G. Mantus, L. E. Nyhoff, M. W. Adelman, R. Fineman, S. Patel, R. Byram, D. N. Gomes, G. Michael, H. Abdullahi, N. Beydoun, B. Panganiban, N. McNair, K. Hellmeister, J. Pitts, J. Winters, J. Kleinhenz, J. Usher, J. B. O'Keefe, A. Piantadosi, J. J. Waggoner, A. Babiker, D. S. Stephens, E. J. Anderson, S. Edupuganti, N. Rouphael, R. Ahmed, J. Wrammert, M. S. Suthar, Infection- and vaccine-induced antibody binding and neutralization of the B.1.351 SARS-CoV-2 variant. *Cell Host Microbe* **29**, 516–521 (2021).
12. K. R. W. Emary, T. Golubchik, P. K. Aley, C. V. Ariani, B. Angus, S. Bibi, B. Blane, D. Bonsall, P. Cicconi, S. Charlton, E. A. Clutterbuck, A. M. Collins, T. Cox, T. C. Darton, C. Dold, A. D. Douglas, C. J. A. Duncan, K. J. Ewer, A. L. Flaxman, S. N. Faust, D. M. Ferreira, S. Feng, A. Finn, P. M. Folegatti, M. Fuskova, E. Galiza, A. L. Goodman, C. M. Green, C. A. Green, M. Greenland, B. Hallis, P. T. Heath, J. Hay, H. C. Hill, D. Jenkin, S. Kerridge, R. Lazarus, V. Libri, P. J. Lillie, C. Ludden, N. G. Marchevsky, A. M. Minassian, A. C. McGregor, Y. F. Mujadidi, D. J. Phillips, E. Plested, K. M. Pollock, H. Robinson, A. Smith, R. Song, M. D. Snape, R. K. Sutherland, E. C. Thomson, M. Toshner, D. P. J. Turner, J. Vekemans, T. L. Villafana, C. J. Williams, A. V. S. Hill, T. Lambe, S. C. Gilbert, M. Voysey, M. N. Ramasamy, A. J. Pollard, Efficacy of ChAdOx1 nCoV-19 (AZD1222) vaccine against SARS-CoV-2 variant of concern 202012/01 (B.1.1.7): An exploratory analysis of a randomised controlled trial. *Lancet* **397**, 1351–1362 (2021).
13. Y. Liu, J. Liu, H. Xia, X. Zhang, C. R. Fontes-Garfias, K. A. Swanson, H. Cai, R. Sarkar, W. Chen, M. Cutler, D. Cooper, S. C. Weaver, A. Muik, U. Sahin, K. U. Jansen, X. Xie, P. R. Dormitzer, P.-Y. Shi, Neutralizing activity of BNT162b2-elicited serum. *N. Engl. J. Med.* **384**, 1466–1468 (2021).

Ng et al., Sci. Transl. Med. **14**, eabn3715 (2022)   27 July 2022

11 of 15

14. P. Wang, M. S. Nair, L. Liu, S. Iketani, Y. Luo, Y. Guo, M. Wang, J. Yu, B. Zhang, P. D. Kwong, B. S. Graham, J. R. Mascola, J. Y. Chang, M. T. Yin, M. Sobieszczyk, C. A. Kyratsous, L. Shapiro, Z. Sheng, Y. Huang, D. D. Ho, Antibody resistance of SARS-CoV-2 variants B.1.351 and B.1.1.7. *Nature* **593**, 130–135 (2021).

15. R. E. Chen, X. Zhang, J. B. Case, E. S. Winkler, Y. Liu, L. A. VanBlargan, J. Liu, J. M. Errico, X. Xie, N. Suryadevara, P. Gilchuk, S. J. Zost, S. Tahan, L. Droit, J. S. Turner, W. Kim, A. J. Schmitz, M. Thapa, D. Wang, A. C. M. Boon, R. M. Presti, J. A. O'Halloran, A. H. J. Kim, P. Deepak, D. Pinto, D. H. Fremont, J. E. Crowe Jr., D. Corti, H. W. Virgin, A. H. Ellebedy, P. Y. Shi, M. S. Diamond, Resistance of SARS-CoV-2 variants to neutralization by monoclonal and serum-derived polyclonal antibodies. *Nat. Med.* **27**, 717–726 (2021).

16. D. T. Skelly, A. C. Harding, J. Gilbert-Jaramillo, M. L. Knight, S. Longet, A. Brown, S. Adele, E. Adland, H. Brown, S. Chinnakannan, T. Donnison, M. Ali, P. Rongkard, M. Pace, P. Zacharopoulou, N. Robinson, A. Csala, C. De Lara, C. L. Hutchings, H. Mehta, L. N. Lee, M. Edmans, C.-P. Hackstein, P. Phalora, W. Li, E. Phillips, T. Malone, A. Ogbe, C. Jay, T. Tipoe, T. Tipton, L. Stafford, A. J. Mentzer, S. A. Johnson, A. Amini, T. Marjot, S. Dimitriadis, B. Simmons, A. Deeks, S. Kerneis, H. Abuelgasim, R. Wilson, S. R. Thomas, A. Watson, A. Alhussni, J. Cutteridge, E. Weeks, L. Denly, K. Lillie, J. Holmes, P. C. Matthews, D. O'Donnell, T. K. Tan, L. Schimanski, K.-Y. A. Huang, P. Rijal, L. Turtle, T. de Silva, A. Richter, C. J. A. Duncan, R. P. Payne, S. C. Moore, J. C. Knight, M. P. Cassar, B. Raman, S. Neubauer, A. Fries, N. P. Talbot, N. Petousis, L.-P. Ho, Y. Peng, T. Dong, S. Camara, S. Marinou, A. Linder, S. Adlou, M. Kasanyinga, A. Bridges-Webb, J. Hill, L. Silva-Reyes, L. Blackwell, J. Frater, P. Goulder, C.-P. Conlon, K. Jeffery, C. Dold, A. J. Pollard, A. Sigal, T. de Oliveira, A. R. Townsend, P. Klenerman, S. J. Dunachie, E. Barnes, M. W. Carroll, W. S. James; Medawar Laboratory Team; OPTIC (Oxford Protective T cell Immunology for COVID-19) Clinical Group; PITCH (Protective Immunity T cells in Health Care Worker) Study Group; C-MORE/PHOSP-C Group, Two doses of SARS-CoV-2 vaccination induce robust immune responses to emerging SARS-CoV-2 variants of concern. *Nat. Commun.* **12**, 5061 (2021).

17. D. Zhou, W. Dejnirattisai, P. Supasa, C. Liu, A. J. Mentzer, H. M. Ginn, Y. Zhao, H. M. E. Duyvesteyn, A. Tuekprakhon, R. Nutalai, B. Wang, G. C. Paesen, C. Lopez-Camacho, J. Slon-Campos, B. Hallis, N. Coombes, K. Bewley, S. Charlton, T. S. Walter, D. Skelly, S. F. Lumley, C. Dold, R. Levin, T. Dong, A. J. Pollard, J. C. Knight, D. Crook, T. Lambe, E. Clutterbuck, S. Bibi, A. Flaxman, S. Bittaye, S. Belij-Rammerstorfer, S. Gilbert, W. James, M. W. Carroll, P. Klenerman, E. Barnes, S. J. Dunachie, E. E. Fry, J. Mongkolsapaya, J. Ren, D. I. Stuart, G. R. Screaton, Evidence of escape of SARS-CoV-2 variant B.1.351 from natural and vaccine induced sera. *Cell* **184**, 2348–2361.e6 (2021).

18. E. C. Wall, M. Wu, R. Harvey, G. Kelly, S. Warchal, C. Sawyer, R. Daniels, L. Adams, P. Hobson, E. Hatipoglu, Y. Ngai, S. Hussain, K. Ambrose, S. Hindmarsh, R. Beale, A. Riddell, S. Gamblin, M. Howell, G. Kassiotis, V. Libri, B. Williams, C. Swanton, S. Gandhi, D. L. Bauer, AZD1222-induced neutralising antibody activity against SARS-CoV-2 Delta VOC. *Lancet* **398**, 207–209 (2021).

19. E. C. Wall, M. Wu, R. Harvey, G. Kelly, S. Warchal, C. Sawyer, R. Daniels, P. Hobson, E. Hatipoglu, Y. Ngai, S. Hussain, J. Nicod, R. Goldstone, K. Ambrose, S. Hindmarsh, R. Beale, A. Riddell, S. Gamblin, M. Howell, G. Kassiotis, V. Libri, B. Williams, C. Swanton, S. Gandhi, D. L. Bauer, Neutralising antibody activity against SARS-CoV-2 VOCs B.1.617.2 and B.1.351 by BNT162b2 vaccination. *Lancet* **397**, 2331–2333 (2021).

20. D. Planas, N. Saunders, P. Maes, F. Guivel-Benhassine, C. Planchais, J. Buchrieser, W.-H. Bolland, F. Porrot, I. Staropoli, F. Lemoine, H. Péré, D. Veyer, J. Puech, J. Rodary, G. Baele, S. Dellicour, J. Raymenants, S. Gorissen, C. Geenen, B. Vanmechelen, T. Wawina-Bokalanga, J. Martí-Carreras, L. Cuypers, A. Sève, S. Hocquelouwx, T. Prazuck, F. A. Rey, E. Simon-Loriere, T. Bruel, H. Mouquet, E. André, O. Schwartz, Considerable escape of SARS-CoV-2 Omicron to antibody neutralization. *Nature* **602**, 671–675 (2022).

21. R. Viana, S. Moyo, D. G. Amoako, H. Tegally, C. Scheepers, C. L. Althaus, U. J. Anyaneji, P. A. Bester, M. F. Boni, M. Chand, W. T. Choga, R. Colquhoun, M. Davids, K. Deforche, D. Doolabh, L. du Plessis, S. Engelbrecht, J. Everatt, J. Giandhari, M. Giovanetti, D. Hardie, V. Hill, N.-Y. Hsiao, A. Iranzadeh, A. Ismail, C. Joseph, R. Joseph, L. Koopile, S. L. K. Pond, M. U. G. Kraemer, L. Kuate-Lere, O. Laguda-Akingba, O. Lesetedi-Mafoko, R. J. Lessells, S. Lockman, A. G. Lucaci, A. Maharaj, B. Mahlangu, T. Maponga, K. Mahlakwane, Z. Makatini, G. Marais, D. Maruapula, K. Masupu, M. Matshaba, S. Mayaphi, N. Mbhele, M. B. Mbulawa, A. Mendes, K. Mlisana, A. Mnguni, T. Mohale, M. Moir, K. Moruisi, M. Mosepele, G. Motsatsi, M. S. Motswaledi, T. Mphoyakgosi, N. Msomi, P. N. Mwangi, Y. Naidoo, N. Ntuli, M. Nyaga, L. Olubayo, S. Pillay, B. Radibe, Y. Ramphal, U. Ramphal, J. E. San, L. Scott, R. Shapiro, L. Singh, P. Smith-Lawrence, W. Stevens, A. Strydom, K. Subramoney, N. Tebeila, D. Tshiabuila, J. Tsui, S. van Wyk, S. Weaver, C. K. Wibmer, E. Wilkinson, N. Wolter, A. E. Zarebski, B. Zuze, D. Goedhals, W. Preiser, F. Treurnicht, M. Venter, C. Williamson, O. G. Pybus, J. Bhiman, A. Glass, D. P. Martin, A. Rambaut, S. Gaseitsiwe, A. von Gottberg, T. de Oliveira, Rapid epidemic expansion of the SARS-CoV-2 Omicron variant in southern Africa. *Nature* **603**, 679–686 (2022).

22. M. Wu, E. C. Wall, E. J. Carr, R. Harvey, H. Townsley, H. V. Mears, L. Adams, S. Kjaer, G. Kelly, S. Warchal, C. Sawyer, C. Kavanagh, C. J. Queval, Y. Ngai, E. Hatipoglu, K. Ambrose, S. Hindmarsh, R. Beale, S. Gamblin, M. Howell, G. Kassiotis, V. Libri, B. Williams, S. Gandhi,

C. Swanton, D. L. Bauer, Three-dose vaccination elicits neutralising antibodies against omicron. *Lancet* **399**, 715–717 (2022).

23. E. Simon-Loriere, O. Schwartz, Towards sARS-CoV-2 serotypes? *Nat. Rev. Microbiol.* **20**, 187–188 (2022).

24. Y. Liu, W. T. Soh, J.-I. Kishikawa, M. Hirose, E. E. Nakayama, S. Li, M. Sasai, T. Suzuki, A. Tada, A. Arakawa, S. Matsuoka, K. Akamatsu, M. Matsuda, C. Ono, S. Torii, K. Kishida, H. Jin, W. Nakai, N. Arase, A. Nakagawa, M. Matsumoto, Y. Nakazaki, Y. Shindo, M. Kohyama, K. Tomii, K. Ohmura, S. Ohshima, T. Okamoto, M. Yamamoto, H. Nakagami, Y. Matsuura, A. Nakagawa, T. Kato, M. Okada, D. M. Standley, T. Shioda, H. Arase, An infectivity-enhancing site on the SARS-CoV-2 spike protein targeted by antibodies. *Cell* **184**, 3452–3466.e18 (2021).

25. W. N. Voss, Y. J. Hou, N. V. Johnson, G. Delidakis, J. E. Kim, K. Javanmardi, A. P. Horton, F. Bartzoka, C. J. Paresi, Y. Tanno, C.-W. Chou, S. A. Abbasi, W. Pickens, K. George, D. R. Boutz, D. M. Towers, J. R. McDaniel, D. Billick, J. Goike, L. Rowe, D. Batra, J. Pohl, J. Lee, S. Gangappa, S. Sambhara, M. Gadush, N. Wang, M. D. Person, B. J. Iverson, J. D. Gollihar, J. Dye, A. Herbert, I. J. Finkelstein, R. S. Baric, J. S. McLellan, G. Georgiou, J. J. Lavinder, G. C. Ippolito, Prevalent, protective, and convergent IgG recognition of SARS-CoV-2 non-RBD spike epitopes. *Science* **372**, 1108–1112 (2021).

26. L. Piccoli, Y.-J. Park, M. A. Tortorici, N. Czudnochowski, A. C. Walls, M. Beltramello, C. Silacci-Fregni, D. Pinto, L. E. Rosen, J. E. Bowen, O. J. Acton, S. Jaconi, B. Guarino, A. Minola, F. Zatta, N. Sprugasci, J. Bassi, A. Peter, A. De Marco, J. C. Nix, F. Mele, S. Jovic, B. F. Rodriguez, S. V. Gupta, F. Jin, G. Piumatti, G. L. Presti, A. F. Pellanda, M. Biggiogero, M. Tarkowski, M. S. Pizzuto, E. Cameroni, C. Havenar-Daughton, M. Smithey, D. Hong, V. Lepori, E. Albanese, A. Ceschi, E. Bernasconi, L. Elzi, P. Ferrari, C. Garzoni, A. Riva, G. Snell, F. Sallusto, K. Fink, H. W. Virgin, A. Lanzavecchia, D. Corti, D. Veesler, Mapping neutralizing and immunodominant sites on the SARS-CoV-2 spike receptor-binding domain by structure-guided high-resolution serology. *Cell* **183**, 1024–1042 (2020).

27. M. E. Garrett, J. Galloway, H. Y. Chu, H. L. Itell, C. I. Stoddard, C. R. Wolf, J. K. Logue, D. McDonald, H. Weight, F. A. I. V. Matsen, J. Overbaugh, High-resolution profiling of pathways of escape for SARS-CoV-2 spike-binding antibodies. *Cell* **184**, 2927–2938.e11 (2021).

28. W. Dejnirattisai, D. Zhou, H. M. Ginn, H. M. E. Duyvesteyn, P. Supasa, J. B. Case, Y. Zhao, T. S. Walter, A. J. Mentzer, C. Liu, B. Wang, G. C. Paesen, J. Slon-Campos, C. López-Camacho, N. M. Kafai, A. L. Bailey, R. E. Chen, B. Ying, C. Thompson, J. Bolton, A. Fyfe, S. Gupta, T. K. Tan, J. Gilbert-Jaramillo, W. James, M. Knight, M. W. Carroll, D. Skelly, C. Dold, Y. Peng, R. Levin, T. Dong, A. J. Pollard, J. C. Knight, P. Klenerman, N. Temperton, D. R. Hall, M. A. Williams, N. G. Paterson, F. K. R. Bertram, C. A. Siebert, D. K. Clare, A. Howe, J. Radecke, Y. Song, A. R. Townsend, K.-Y. A. Huang, E. E. Fry, J. Mongkolsapaya, M. S. Diamond, J. Ren, D. I. Stuart, G. R. Screaton, The antigenic anatomy of SARS-CoV-2 receptor binding domain. *Cell* **184**, 2183–2200 (2021).

29. A. S. Heffron, S. J. McIlwain, M. F. Amjadi, D. A. Baker, S. Khullar, T. Armbrust, P. J. Halfmann, Y. Kawaoka, A. K. Sethi, A. C. Palmenberg, M. A. Shelef, D. H. O'Connor, I. M. Ong, The landscape of antibody binding in SARS-CoV-2 infection. *PLoS Biol.* **19**, e3001265 (2021).

30. C. Graham, J. Seow, I. Huettner, H. Khan, N. Kouphou, S. Acors, H. Winstone, S. Pickering, R. P. Galao, L. Dupont, M. J. Lista, J. M. Jimenez-Guardeño, A. G. Laing, Y. Wu, M. Joseph, L. Muir, M. J. van Gils, W. M. Ng, H. M. E. Duyvesteyn, Y. Zhao, T. A. Bowden, M. Shankar-Hari, A. Rosa, P. Cherepanov, L. E. McCoy, A. C. Hayday, S. J. D. Neil, M. H. Malim, K. J. Doores, Neutralization potency of monoclonal antibodies recognizing dominant and subdominant epitopes on SARS-CoV-2 Spike is impacted by the B.1.1.7 variant. *Immunity* **54**, 1276–1289 (2021).

31. F. Amanat, M. Thapa, T. Lei, S. M. Sayed Ahmed, D. C. Adelsberg, J. M. Carreno, S. Strohmeier, A. J. Schmitz, S. Zafar, J. Q. Zhou, W. Rijnink, H. Alshammary, N. Borcherding, A. G. Reiche, K. Srivastava, E. M. Sordillo, H. van Bakel, J. S. Turner, G. Bajic, V. Simon, A. H. Ellebedy, F. Krammer, SARS-CoV-2 mRNA vaccination induces functionally diverse antibodies to NTD, RBD and S2. *Cell* **184**, 3936–3948.e10 (2021).

32. K. W. Ng, N. Faulkner, G. H. Cornish, A. Rosa, R. Harvey, S. Hussain, R. Ulferts, C. Earl, A. G. Wrobel, D. J. Benton, C. Roustan, W. Bolland, R. Thompson, A. Agua-Doce, P. Hobson, J. Heaney, H. Rickman, S. Paraskevopoulou, C. F. Houlihan, K. Thomson, E. Sanchez, G. Y. Shin, M. J. Spyer, D. Joshi, N. O'Reilly, P. A. Walker, S. Kjaer, A. Riddell, C. Moore, B. R. Jebson, M. Wilkinson, L. R. Marshall, E. C. Rosser, A. Radziszewska, H. Peckham, C. Ciurtin, L. R. Wedderburn, R. Beale, C. Swanton, S. Gandhi, B. Stockinger, J. McCauley, S. J. Gamblin, L. E. McCoy, P. Cherepanov, E. Nastouli, G. Kassiotis, Preexisting and de novo humoral immunity to SARS-CoV-2 in humans. *Science* **370**, 1339–1343 (2020).

33. E. Shrock, E. Fujimura, T. Kula, R. T. Timms, I.-H. Lee, Y. Leng, M. L. Robinson, B. M. Sie, M. Z. Li, Y. Chen, J. Logue, A. Zuiani, D. McCulloch, F. J. N. Lelis, S. Henson, D. R. Monaco, M. Travers, S. Habibi, W. A. Clarke, P. Caturegli, O. Laeyendecker, A. Piechocka-Trocha, J. Li, A. Khatri, H. Y. Chu, A.-C. Villani, K. Kays, M. B. Goldberg, N. Hacohen, M. R. Filbin, X. G. Yu, B. D. Walker, D. R. Wesemann, H. B. Larman, J. A. Lederer, S. J. Elledge, Viral epitope profiling of COVID-19 patients reveals cross-reactivity and correlates of severity. *Science* **370**, eabd4250 (2020).

34. W. R. Morgenlander, S. N. Henson, D. R. Monaco, A. Chen, K. Littlefield, E. M. Bloch, E. Fujimura, I. Ruczinski, A. R. Crowley, H. Natarajan, S. E. Butler, J. A. Weiner, M. Z. Li, T. S. Bonny, S. E. Benner, A. Balagopal, D. Sullivan, S. Shoham, T. C. Quinn, S. Eshleman, A. Casadevall, A. D. Redd, O. Laeyendecker, M. E. Ackerman, A. Pekosz, S. J. Elledge, M. L. Robinson, A. A. R. Tobian, H. B. Larman, Antibody responses to endemic coronaviruses modulate COVID-19 convalescent plasma functionality. *J. Clin. Invest.* **131**, e146927 (2021).

35. J. T. Ladner, S. N. Henson, A. S. Boyle, A. L. Engelbrektson, Z. W. Fink, F. Rahee, J. D'Ambrozio, K. E. Schaecher, M. Stone, W. Dong, S. Dadwal, J. Yu, M. A. Caligiuri, P. Cieplak, M. Bjørås, M. H. Fenstad, S. A. Nordbø, D. E. Kainov, N. Muranaka, M. S. Chee, S. A. Shiryaev, J. A. Altin, Epitope-resolved profiling of the SARS-CoV-2 antibody response identifies cross-reactivity with endemic human coronaviruses. *Cell Rep. Med.* **2**, 100189 (2021).

36. P. Nguyen-Contant, A. K. Embong, P. Kanagaiah, F. A. Chaves, H. Yang, A. R. Branche, D. J. Topham, M. Y. Sangster, S protein-reactive IgG and memory B cell production after human SARS-CoV-2 infection includes broad reactivity to the S2 subunit. *MBio* **11**, e01991–e01920 (2020).

37. T. Dangi, N. Palacio, S. Sanchez, M. Park, J. Class, L. Visvabharathy, T. Ciucci, I. J. Koralnik, J. M. Richner, P. Penaloza-MacMaster, Cross-protective immunity following coronavirus vaccination and coronavirus infection. *J. Clin. Invest.* **131**, e151969 (2021).

38. K. M. Lip, S. Shen, X. Yang, C. T. Keng, A. Zhang, H. L. Oh, Z. H. Li, L. A. Hwang, C. F. Chou, B. C. Fielding, T. H. Tan, J. Mayrhofer, F. G. Falkner, F. Fu, S. G. Lim, W. Hong, Y. J. Tan, Monoclonal antibodies targeting the HR2 domain and the region immediately upstream of the HR2 of the S protein neutralize in vitro infection of severe acute respiratory syndrome coronavirus. *J. Virol.* **80**, 941–950 (2006).

39. H. A. Elshabrawy, M. M. Coughlin, S. C. Baker, B. S. Prabhakar, Human monoclonal antibodies against highly conserved HR1 and HR2 domains of the SARS-CoV spike protein are more broadly neutralizing. *PLOS ONE* **7**, e50366 (2012).

40. J. Duan, X. Yan, X. Guo, W. Cao, W. Han, C. Qi, J. Feng, D. Yang, G. Gao, G. Jin, A human SARS-CoV neutralizing antibody against epitope on S2 protein. *Biochem. Biophys. Res. Commun.* **333**, 186–193 (2005).

41. C. Wang, R. van Haperen, J. Gutiérrez-Álvarez, W. Li, N. M. A. Okba, I. Albulescu, I. Widjaja, B. van Dieren, R. Fernandez-Delgado, I. Sola, D. L. Hurdiss, O. Daramola, F. Grosveld, F. J. M. van Kuppeveld, B. L. Haagmans, L. Enjuanes, D. Drabek, B. J. Bosch, A conserved immunogenic and vulnerable site on the coronavirus spike protein delineated by cross-reactive monoclonal antibodies. *Nat. Commun.* **12**, 1715 (2021).

42. X. Chi, R. Yan, J. Zhang, G. Zhang, Y. Zhang, M. Hao, Z. Zhang, P. Fan, Y. Dong, Y. Yang, Z. Chen, Y. Guo, J. Zhang, Y. Li, X. Song, Y. Chen, L. Xia, L. Fu, L. Hou, J. Xu, C. Yu, J. Li, Q. Zhou, W. Chen, A neutralizing human antibody binds to the N-terminal domain of the Spike protein of SARS-CoV-2. *Science* **369**, 650–655 (2020).

43. G. Song, W.-t. He, S. Callaghan, F. Anzanello, D. Huang, J. Ricketts, J. L. Torres, N. Beutler, L. Peng, S. Vargas, J. Cassell, M. Parren, L. Yang, C. Ignacio, D. M. Smith, J. E. Voss, D. Nemazee, A. B. Ward, T. Rogers, D. R. Burton, R. Andrabi, Cross-reactive serum and memory B-cell responses to spike protein in SARS-CoV-2 and endemic coronavirus infection. *Nat. Commun.* **12**, 2938 (2021).

44. M. M. Sauer, M. A. Tortorici, Y. J. Park, A. C. Walls, L. Homad, O. J. Acton, J. E. Bowen, C. Wang, X. Xiong, W. de van der Schueren, J. Quispe, B. G. Hoffstrom, B. J. Bosch, A. T. McGuire, D. Veesler, Structural basis for broad coronavirus neutralization. *Nat. Struct. Mol. Biol.* **28**, 478–486 (2021).

45. D. Pinto, M. M. Sauer, N. Czudnochowski, J. S. Low, M. A. Tortorici, M. P. Housley, J. Noack, A. C. Walls, J. E. Bowen, B. Guarino, L. E. Rosen, J. di Iulio, J. Jerak, H. Kaiser, S. Islam, S. Jaconi, N. Sprugasci, K. Culap, R. Abdelnabi, C. Foo, L. Coelmont, I. Bartha, S. Bianchi, C. Silacci-Fregni, J. Bassi, R. Marzi, E. Vetti, A. Cassotta, A. Ceschi, P. Ferrari, P. E. Cippà, O. Giannini, S. Ceruti, C. Garzoni, A. Riva, F. Benigni, E. Cameroni, L. Piccoli, M. S. Pizzuto, M. Smithey, D. Hong, A. Telenti, F. A. Lempp, J. Neyts, C. Havenar-Daughton, A. Lanzavecchia, F. Sallusto, G. Snell, H. W. Virgin, M. Beltramello, D. Corti, D. Veesler, Broad betacoronavirus neutralization by a stem helix-specific human antibody. *Science* **373**, 1109–1116 (2021).

46. Y. Huang, A. W. Nguyen, C.-L. Hsieh, R. Silva, O. S. Olaluwoye, R. E. Wilen, T. S. Kaoud, L. R. Azouz, A. N. Qerqez, K. C. Le, A. L. Bohanon, A. M. DiVenere, Y. Liu, A. G. Lee, D. Amengor, K. N. Dalby, S. D'Arcy, J. S. McLellan, J. A. Maynard, Identification of a conserved neutralizing epitope present on spike proteins from all highly pathogenic coronaviruses. *bioRxiv* 2021.2001.2031.428824 (2021).

47. K. W. Ng, N. Faulkner, A. G. Wrobel, S. J. Gamblin, G. Kassiotis, Heterologous humoral immunity to human and zoonotic coronaviruses: Aiming for the achilles' heel. *Semin. Immunol.* **55**, 101507–101518 (2021).

48. W. W. Leitner, H. Ying, N. P. Restifo, DNA and RNA-based vaccines: Principles, progress and prospects. *Vaccine* **18**, 765–777 (1999).

49. N. Faulkner, K. W. Ng, M. Y. Wu, R. Harvey, M. Margaritis, S. Paraskevopoulou, C. Houlihan, S. Hussain, M. Greco, W. Bolland, S. Warchal, J. Heaney, H. Rickman, M. Spyer, D. Frampton, M. Byott, T. de Oliveira, A. Sigal, S. Kjaer, C. Swanton, S. Gandhi, R. Beale, S. J. Gamblin, J. W. McCauley, R. S. Daniels, M. Howell, D. Bauer, E. Nastouli, G. Kassiotis, Reduced antibody cross-reactivity following infection with B.1.1.7 than with parental SARS-CoV-2 strains. *eLife* **10**, e69317 (2021).

50. D. S. Khoury, D. Cromer, A. Reynaldi, T. E. Schlub, A. K. Wheatley, J. A. Juno, K. Subbarao, S. J. Kent, J. A. Triccas, M. P. Davenport, Neutralizing antibody levels are highly predictive of immune protection from symptomatic SARS-CoV-2 infection. *Nat. Med.* **27**, 1205–1211 (2021).

51. S. Feng, D. J. Phillips, T. White, H. Sayal, P. K. Aley, S. Bibi, C. Dold, M. Fuskova, S. C. Gilbert, I. Hirsch, H. E. Humphries, B. Jepson, E. J. Kelly, E. Plested, K. Shoemaker, K. M. Thomas, J. Vekemans, T. L. Villafana, T. Lambe, A. J. Pollard, M. Voysey, S. Adlou, L. Allen, B. Angus, R. Anslow, M.-C. Asselin, N. Baker, P. Baker, T. Barlow, A. Beveridge, K. R. Bewley, P. Brown, E. Brunt, K. R. Buttigieg, S. Camara, S. Charlton, E. Chiplin, P. Cicconi, E. A. Clutterbuck, A. M. Collins, N. S. Coombes, S. A. C. Clemens, M. Davison, T. Demissie, T. Dinesh, A. D. Douglas, C. J. A. Duncan, K. R. W. Emary, K. J. Ewer, S. Felle, D. M. Ferreira, A. Finn, P. M. Folegatti, R. Fothergill, S. Fraser, L. Garlant, L. Gatcombe, K. J. Godwin, A. L. Goodman, C. A. Green, B. Hallis, T. C. Hart, P. T. Heath, H. Hill, A. V. S. Hill, D. Jenkin, M. Kasanyinga, S. Kerridge, C. Knight, S. Leung, V. Libri, P. J. Lillie, S. Marinou, J. McGlashan, A. C. McGregor, L. McInroy, A. M. Minassian, Y. F. Mujadidi, E. J. Penn, C. J. Petropoulos, K. M. Pollock, P. C. Proud, S. Provstgaard-Morys, D. Rajapaska, M. N. Ramasamy, K. Sanders, I. Shaik, N. Singh, A. Smith, M. D. Snape, R. Song, S. Shrestha, R. K. Sutherland, E. C. Thomson, D. P. J. Turner, A. Webb-Bridges, T. Wrin, C. J. Williams; the Oxford COVID Vaccine Trial Group, Correlates of protection against symptomatic and asymptomatic SARS-CoV-2 infection. *Nat. Med.* **27**, 2032–2040 (2021).

52. P. B. Gilbert, D. C. Montefiori, A. B. McDermott, Y. Fong, D. Benkeser, W. Deng, H. Zhou, C. R. Houchens, K. Martins, L. Jayashankar, F. Castellino, B. Flach, B. C. Lin, S. O'Connell, C. McDanal, A. Eaton, M. Sarzotti-Kelsoe, Y. Lu, C. Yu, B. Borate, L. W. P. van der Laan, N. S. Hejazi, C. Huynh, J. Miller, H. M. El Sahly, L. R. Baden, M. Baron, L. De La Cruz, C. Gay, S. Kalams, C. F. Kelley, M. P. Andrasik, J. G. Kublin, L. Corey, K. M. Neuzil, L. N. Carpp, R. Pajon, D. Follmann, R. O. Donis, R. A. Koup, Immune correlates analysis of the mRNA-1273 COVID-19 vaccine efficacy clinical trial. *Science* **375**, 43–50 (2022).

53. P. B. McCray Jr., L. Pewe, C. Wohlford-Lenane, M. Hickey, L. Manzel, L. Shi, J. Netland, H. P. Jia, C. Halabi, C. D. Sigmund, D. K. Meyerholz, P. Kirby, D. C. Look, S. Perlman, Lethal infection of K18-hACE2 mice infected with severe acute respiratory syndrome coronavirus. *J. Virol.* **81**, 813–821 (2007).

54. A. H. Ellebedy, R. Ahmed, Re-engaging cross-reactive memory B cells: The influenza puzzle. *Front. Immunol.* **3**, 53 (2012).

55. P. J. Halfmann, S. Iida, K. Iwatsuki-Horimoto, T. Maemura, M. Kiso, S. M. Scheaffer, T. L. Darling, A. Joshi, S. Loeber, G. Singh, S. L. Foster, B. Ying, J. B. Case, Z. Chong, B. Whitener, J. Moliva, K. Floyd, M. Ujie, N. Nakajima, M. Ito, R. Wright, R. Uraki, P. Warang, M. Gagne, R. Li, Y. Sakai-Tagawa, Y. Liu, D. Larson, J. E. Osorio, J. P. Hernandez-Ortiz, A. R. Henry, K. Ciouderis, K. R. Florek, M. Patel, A. Odle, L.-Y. R. Wong, A. C. Bateman, Z. Wang, V.-V. Edara, Z. Chong, J. Franks, T. Jeevan, T. Fabrizio, J. DeBeauchamp, L. Kercher, P. Seiler, A. S. Gonzalez-Reiche, E. M. Sordillo, L. A. Chang, H. van Bakel, V. Simon, B. Alburquerque, H. Alshammary, A. A. Amoako, S. Aslam, R. Banu, C. Cognigni, M. Espinoza-Moraga, K. Farrugia, A. van de Guchte, Z. Khalil, M. Laporte, I. Mena, A. E. Paniz-Mondolfi, J. Polanco, A. Rooker, J. L. Sominsky, D. C. Douek, N. J. Sullivan, L. B. Thackray, H. Ueki, S. Yamayoshi, M. Imai, S. Perlman, R. J. Webby, R. A. Seder, M. S. Suthar, A. García-Sastre, M. Schotsaert, A. Suzuki, A. C. M. Boon, M. S. Diamond, Y. Kawaoka; Consortium Mount Sinai Pathogen Surveillance (PSP) study group, SARS-CoV-2 Omicron virus causes attenuated disease in mice and hamsters. *Nature* **603**, 687–692 (2022).

56. R. Abdelnabi, C. S. Foo, X. Zhang, V. Lemmens, P. Maes, B. Slechten, J. Raymenants, E. André, B. Weynand, K. Dallmeier, J. Neyts, The omicron (B.1.1.529) SARS-CoV-2 variant of concern does not readily infect Syrian hamsters. *Antiviral Res.* **198**, 105253 (2022).

57. D. Planas, T. Bruel, L. Grzelak, F. Guivel-Benhassine, I. Staropoli, F. Porrot, C. Planchais, J. Buchrieser, M. M. Rajah, E. Bishop, M. Albert, F. Donati, M. Prot, S. Behillil, V. Enouf, M. Maquart, M. Smati-Lafarge, E. Varon, F. Schortgen, L. Yahyaoui, M. Gonzalez, J. De Sèze, H. Péré, D. Veyer, A. Sève, E. Simon-Lorière, S. Fafi-Kremer, K. Stefic, H. Mouquet, L. Hocqueloux, S. van der Werf, T. Prazuck, O. Schwartz, Sensitivity of infectious SARS-CoV-2 B.1.1.7 and B.1.351 variants to neutralizing antibodies. *Nat. Med.* **27**, 917–924 (2021).

58. C. K. Wibmer, F. Ayres, T. Hermanus, M. Madzivhandila, P. Kgagudi, B. Oosthuysen, B. E. Lambson, T. de Oliveira, M. Vermeulen, K. van der Berg, T. Rossouw, M. Boswell, V. Ueckermann, S. Meiring, A. von Gottberg, C. Cohen, L. Morris, J. N. Bhiman, P. L. Moore, SARS-CoV-2 501Y.V2 escapes neutralization by South African COVID-19 donor plasma. *Nat. Med.* **27**, 622–625 (2021).

59. S. Cele, I. Gazy, L. Jackson, S.-H. Hwa, H. Tegally, G. Lustig, J. Giandhari, S. Pillay, E. Wilkinson, Y. Naidoo, F. Karim, Y. Ganga, K. Khan, M. Bernstein, A. B. Balazs, B. I. Gosnell, W. Hanekom, M.-Y. S. Moosa, R. J. Lessells, T. de Oliveira, A. Sigal, S. A. Ngs, C.-K. Team, Escape of SARS-CoV-2 501Y.V2 from neutralization by convalescent plasma. *Nature* **593**, 142–146 (2021).

60. J. C. Brown, D. H. Goldhill, J. Zhou, T. P. Peacock, R. Frise, N. Goonawardane, L. Baillon, R. Kugathasan, A. Pinto, P. F. McKay, J. Hassard, M. Moshe, A. Singanayagam, T. Burgoyne, W. S. Barclay, Increased transmission of SARS-CoV-2 lineage B.1.1.7 (VOC 2020212/01) is not accounted for by a replicative advantage in primary airway cells or antibody escape. *bioRxiv* 2021.2002.2024.432576 (2021).

61. L. Guo, Y. Wang, L. Kang, Y. Hu, L. Wang, J. Zhong, H. Chen, L. Ren, X. Gu, G. Wang, C. Wang, X. Dong, C. Wu, L. Han, Y. Wang, G. Fan, X. Zou, H. Li, J. Xu, Q. Jin, B. Cao, J. Wang, Cross-reactive antibody against human coronavirus OC43 spike protein correlates with disease severity in COVID-19 patients: A retrospective study. *Emerg. Microbes Infect.* **10**, 664–676 (2021).

62. M. Sagar, K. Reifler, M. Rossi, N. S. Miller, P. Sinha, L. White, J. P. Mizgerd, Recent endemic coronavirus infection is associated with less severe COVID-19. *J. Clin. Invest.* **131**, e143380 (2020).

63. L. Henss, T. Scholz, C. von Rhein, I. Wieters, F. Borgans, F. J. Eberhardt, K. Zacharowski, S. Ciesek, G. Rohde, M. Vehreschild, C. Stephan, T. Wolf, H. Hofmann-Winkler, H. Scheiblauer, B. S. Schnierle, Analysis of humoral immune responses in SARS-CoV-2 infected patients. *J Infect Dis* **223**, 56–61 (2020).

64. T. Zohar, C. Loos, S. Fischinger, C. Atyeo, C. Wang, M. D. Slein, J. Burke, J. Yu, J. Feldman, B. M. Hauser, T. Caradonna, A. G. Schmidt, Y. Cai, H. Streeck, E. T. Ryan, D. H. Barouch, R. C. Charles, D. A. Lauffenburger, G. Alter, Compromised humoral functional evolution tracks with SARS-CoV-2 mortality. *Cell* **183**, 1508–1519.e12 (2020).

65. Y. Wang, L. Zhang, L. Sang, F. Ye, S. Ruan, B. Zhong, T. Song, A. N. Alshukairi, R. Chen, Z. Zhang, M. Gan, A. Zhu, Y. Huang, L. Luo, C. K. P. Mok, M. M. Al Gethamy, H. Tan, Z. Li, X. Huang, F. Li, J. Sun, Y. Zhang, L. Wen, Y. Li, Z. Chen, Z. Zhuang, J. Zhuo, C. Chen, L. Kuang, J. Wang, H. Lv, Y. Jiang, M. Li, Y. Lin, Y. Deng, L. Tang, J. Liang, J. Huang, S. Perlman, N. Zhong, J. Zhao, J. S. M. Peiris, Y. Li, J. Zhao, Kinetics of viral load and antibody response in relation to COVID-19 severity. *J. Clin. Invest.* **130**, 5235–5244 (2020).

66. P. Kaplonek, C. Wang, Y. Bartsch, S. Fischinger, J. G. Matthew, K. Bowman, J. Kang, D. Dayal, P. Martin, P. N. Radoslaw, A.-C. Villani, C.-L. Hsieh, C. C. Nicole, L. K. G. Anna, I. Gushterova, K. K. Hargun, J. L. Thomas, M. L.-P. Kendall, M. L. Brendan, L. L. Carl, K. Manakongtreecheep, D. M. Justin, N. M. Brenna, M. Rojas-Lopez, C. R. Brian, N. Sharma, J. Tantivit, F. T. Molly, M. Sade-Feldman, J. Feldman, B. Julg, J. N. Eric, R. M. Elon, S. M. Anil, S. F. Eric, S. M. Jason, A. Schmidt, B. G. Marcia, R. F. Michael, N. Hacohen, A. L. Douglas, G. Alter, Early cross-coronavirus reactive signatures of humoral immunity against COVID-19. *Sci. Immunol.* **6**, eabj2901 (2021).

67. M. Aguilar-Bretones, B. M. Westerhuis, M. P. Raadsen, E. de Bruin, F. D. Chandler, N. M. Okba, B. L. Haagmans, T. Langerak, H. Endeman, J. P. van den Akker, D. A. Gommers, E. C. van Gorp, C. H. GeurtsvanKessel, R. D. de Vries, R. A. Fouchier, B. H. Rockx, M. P. Koopmans, G. P. van Nierop, Seasonal coronavirus-specific B cells with limited SARS-CoV-2 cross-reactivity dominate the IgG response in severe COVID-19. *J. Clin. Invest.* **131**, e150613 (2021).

68. T. Aydillo, A. Rombauts, D. Stadlbauer, S. Aslam, G. Abelenda-Alonso, A. Escalera, F. Amanat, K. Jiang, F. Krammer, J. Carratala, A. García-Sastre, Immunological imprinting of the antibody response in COVID-19 patients. *Nat. Commun.* **12**, 3781 (2021).

69. A. L. McNaughton, R. S. Paton, M. Edmans, J. Youngs, J. Wellens, P. Phalora, A. Fyfe, S. Belij-Rammerstorfer, J. S. Bolton, J. Ball, G. Carnell, W. Dejnirattisai, C. Dold, D. W. Eyre, P. Hopkins, A. Howarth, K. Kooblall, H. Klim, S. Leaver, L. Lee, C. López-Camacho, S. F. Lumley, D. Macallan, A. J. Mentzer, N. Provine, J. Ratcliff, J. Slon-Compos, D. Skelly, L. Stolle, P. Supasa, N. Temperton, C. Walker, B. Wang, D. Wyncoll, P. Simmonds, T. Lambe, K. Baillie, M. G. Semple, P. I. Openshaw, U. Obolski, M. Turner, M. Carroll, J. Mongkolsapaya, G. Screaton, S. H. Kennedy, L. Jarvis, E. Barnes, S. Dunachie, J. Lourenço, P. C. Matthews, T. Bicanic, P. Klenerman, S. Gupta, C. P. Thompson, Fatal COVID-19 outcomes are associated with an antibody response targeting epitopes shared with endemic coronaviruses. *JCI Insight* **7**, e156372 (2022).

70. S. A. Lapp, V. V. Edara, A. Lu, L. Lai, L. Hussaini, A. Chahroudi, L. J. Anderson, M. S. Suthar, E. J. Anderson, C. A. Rostad, Original antigenic sin responses to Betacoronavirus spike proteins are observed in a mouse model, but are not apparent in children following SARS-CoV-2 infection. *PLOS ONE* **16**, e0256482 (2021).

71. A. Z. Wec, D. Wrapp, A. S. Herbert, D. P. Maurer, D. Haslwanter, M. Sakharkar, R. K. Jangra, M. E. Dieterle, A. Lilov, D. Huang, L.-V. Tse, N. V. Johnson, C.-L. Hsieh, N. Wang, J. H. Nett, E. Champney, I. Burnina, M. Brown, S. Lin, M. Sinclair, C. Johnson, S. Pudi, R. Bortz, A. S. Wirchnianski, E. Laudermilch, C. Florez, J. M. Fels, C. M. O'Brien, B. S. Graham, D. Nemazee, D. R. Burton, R. S. Baric, J. E. Voss, K. Chandran, J. M. Dye, J. S. McLellan, L. M. Walker, Broad neutralization of SARS-related viruses by human monoclonal antibodies. *Science* **369**, 731–736 (2020).

72. Y. Guo, S. Sun, K. Wang, S. Zhang, W. Zhu, Z. Chen, Elicitation of immunity in mice after immunization with the S2 subunit of the severe acute respiratory syndrome coronavirus. *DNA Cell Biol.* **24**, 510–515 (2005).

73. C. T. Keng, A. Zhang, S. Shen, K. M. Lip, B. C. Fielding, T. H. Tan, C. F. Chou, C. B. Loh, S. Wang, J. Fu, X. Yang, S. G. Lim, W. Hong, Y. J. Tan, Amino acids 1055 to 1192 in the S2

region of severe acute respiratory syndrome coronavirus S protein induce neutralizing antibodies: Implications for the development of vaccines and antiviral agents. *J. Virol.* **79**, 3289–3296 (2005).

74. X. Ma, F. Zou, F. Yu, R. Li, Y. Yuan, Y. Zhang, X. Zhang, J. Deng, T. Chen, Z. Song, Y. Qiao, Y. Zhan, J. Liu, J. Zhang, X. Zhang, Z. Peng, Y. Li, Y. Lin, L. Liang, G. Wang, Y. Chen, Q. Chen, T. Pan, X. He, H. Zhang, Nanoparticle vaccines based on the receptor binding domain (RBD) and heptad repeat (HR) of SARS-CoV-2 elicit robust protective immune responses. *Immunity* **53**, 1315–1330.e9 (2020).

75. C.-L. Hsieh, A. P. Werner, S. R. Leist, L. J. Stevens, E. Falconer, J. A. Goldsmith, C.-W. Chou, O. M. Abiona, A. West, K. Westendorf, K. Muthuraman, E. J. Fritch, K. H. Dinnon III, A. Schäfer, M. R. Denison, J. D. Chappell, R. S. Baric, B. S. Graham, K. S. Corbett, J. S. McLellan, Stabilized coronavirus spike stem elicits a broadly protective antibody. *Cell Rep.* **37**, 109929 (2021).

76. D. L. N. F. Maeda, D. Tian, H. Yu, N. Dar, V. Rajasekaran, S. Meng, H. M. Mahsoub, H. Sooryanarain, B. Wang, C. L. Heffron, A. Hassebroek, T. LeRoith, X.-J. Meng, S. L. Zeichner, Killed whole-genome reduced-bacteria surface-expressed coronavirus fusion peptide vaccines protect against disease in a porcine model. *Proc. Natl. Acad. Sci. U.S.A.* **118**, e2025622118 (2021).

77. S. A. Kemp, D. A. Collier, R. P. Datir, I. Ferreira, S. Gayed, A. Jahun, M. Hosmillo, C. Rees-Spear, P. Mlcochova, I. U. Lumb, D. J. Roberts, A. Chandra, N. Temperton, K. Sharrocks, E. Blane, Y. Modis, K. Leigh, J. Briggs, M. van Gils, K. G. C. Smith, J. R. Bradley, C. Smith, R. Doffinger, L. Ceron-Gutierrez, G. Barcenas-Morales, D. Pollock, R. A. Goldstein, A. Smielewska, J. P. Skittrall, T. Gouliouris, I. G. Goodfellow, E. Gkrania-Klotsas, C. J. R. Illingworth, L. E. McCoy, R. K. Gupta, SARS-CoV-2 evolution during treatment of chronic infection. *Nature* **592**, 277–282 (2021).

78. H. Tegally, M. Ramuth, D. Amoako, C. Scheepers, E. Wilkinson, M. Giovanetti, R. J. Lessells, J. Giandhari, A. Ismail, D. Martin, E. J. San, M. Crawford, R. S. Daniels, R. Harvey, S. Bahadoor, J. Sonoo, M. Timol, L. Veerapa-Mangroo, A. V. Gottberg, J. N. Bhiman, T. de Oliveira, S. Manraj, Genomic epidemiology of SARS-CoV-2 in Mauritius reveals a new wave of infections dominated by the B.1.1.318, a variant under investigation. *medRxiv* 2021.2006.2016.21259017 (2021).

79. A. A. Cohen, P. N. P. Gnanapragasam, Y. E. Lee, P. R. Hoffman, S. Ou, L. M. Kakutani, J. R. Keeffe, H. J. Wu, M. Howarth, A. P. West, C. O. Barnes, M. C. Nussenzweig, P. J. Bjorkman, Mosaic nanoparticles elicit cross-reactive immune responses to zoonotic coronaviruses in mice. *Science* **371**, 735–741 (2021).

80. A. C. Walls, M. C. Miranda, A. Schäfer, M. N. Pham, A. Greaney, P. S. Arunachalam, M. J. Navarro, M. A. Tortorici, K. Rogers, M. A. O'Connor, L. Shireff, D. E. Ferrell, J. Bowen, N. Brunette, E. Kepl, S. K. Zepeda, T. Starr, C. L. Hsieh, B. Fiala, S. Wrenn, D. Pettie, C. Sydeman, K. R. Sprouse, M. Johnson, A. Blackstone, R. Ravichandran, C. Ogohara, L. Carter, S. W. Tilles, R. Rappuoli, S. R. Leist, D. R. Martinez, M. Clark, R. Tisch, D. T. O'Hagan, R. Van Der Most, W. C. Van Voorhis, D. Corti, J. S. McLellan, H. Kleanthous, T. P. Sheahan, K. D. Smith, D. H. Fuller, F. Villinger, J. Bloom, B. Pulendran, R. S. Baric, N. P. King, D. Veesler, Elicitation of broadly protective sarbecovirus immunity by receptor-binding domain nanoparticle vaccines. *Cell* **184**, 5432–5447 (2021).

81. K. O. Saunders, E. Lee, R. Parks, D. R. Martinez, D. Li, H. Chen, R. J. Edwards, S. Gobeil, M. Barr, K. Mansouri, S. M. Alam, L. L. Sutherland, F. Cai, A. M. Sanzone, M. Berry, K. Manne, K. W. Bock, M. Minai, B. M. Nagata, A. B. Kapingidza, M. Azoitei, L. V. Tse, T. D. Scobey, R. L. Spreng, R. W. Rountree, C. T. DeMarco, T. N. Denny, C. W. Woods, E. W. Petzold, J. Tang, T. H. Oguin, G. D. Sempowski, M. Gagne, D. C. Douek, M. A. Tomai, C. B. Fox, R. Seder, K. Wiehe, D. Weissman, N. Pardi, H. Golding, S. Khurana, P. Acharya, H. Andersen, M. G. Lewis, I. N. Moore, D. C. Montefiori, R. S. Baric, B. F. Haynes, Neutralizing antibody vaccine for pandemic and pre-emergent coronaviruses. *Nature* **594**, 553–559 (2021).

82. H. A. D. King, M. G. Joyce, I. Lakhal-Naouar, A. Ahmed, C. M. Cincotta, S. Subra, K. K. Peachman, H. R. Hack, R. E. Chen, P. V. Thomas, W. H. Chen, R. S. Sankhala, A. Hajduczki, E. J. Martinez, C. E. Peterson, W. C. Chang, M. Choe, C. Smith, J. A. Headley, H. A. Elyard, A. Cook, A. Anderson, K. M. Wuertz, M. Dong, I. Swafford, J. B. Case, J. R. Currier, K. G. Lal, M. F. Amare, V. Dussupt, S. Molnar, S. P. Daye, X. Zeng, E. K. Barkei, K. Alfson, H. M. Staples, R. Carrion, S. J. Krebs, D. Paquin-Proulx, N. Karasavvas, V. R. Polonis, L. L. Jagodzinski, S. Vasan, P. T. Scott, Y. Huang, M. S. Nair, D. D. Ho, N. de Val, M. S. Diamond, M. G. Lewis, M. Rao, G. R. Matyas, G. D. Gromowski, S. A. Peel, N. L. Michael, K. Modjarrad, D. L. Bolton, Efficacy and breadth of adjuvanted SARS-CoV-2 receptor-binding domain nanoparticle vaccine in macaques. *Proc. Natl. Acad. Sci. U.S.A.* **118**, e2106433118 (2021).

83. K. M. Wuertz, E. K. Barkei, W. H. Chen, E. J. Martinez, I. Lakhal-Naouar, L. L. Jagodzinski, D. Paquin-Proulx, G. D. Gromowski, I. Swafford, A. Ganesh, M. Dong, X. Zeng, P. V. Thomas, R. S. Sankhala, A. Hajduczki, C. E. Peterson, C. Kuklis, S. Soman, L. Wieczorek, M. Zemil, A. Anderson, J. Darden, H. Hernandez, H. Grove, V. Dussupt, H. Hack, R. de la Barrera, S. Zarling, J. F. Wood, J. W. Froude, M. Gagne, A. R. Henry, E. B. Mokhtari, P. Mudvari, S. J. Krebs, A. S. Pekosz, J. R. Currier, S. Kar, M. Porto, A. Winn, K. Radzyminski, M. G. Lewis, S. Vasan, M. Suthar, V. R. Polonis, G. R. Matyas, E. A. Boritz, D. C. Douek, R. A. Seder, S. P. Daye, M. Rao, S. A. Peel, M. G. Joyce, D. L. Bolton, N. L. Michael,

Ng et al., *Sci. Transl. Med.* **14**, eabn3715 (2022)   27 July 2022

14 of 15

K. Modjarrad, A SARS-CoV-2 spike ferritin nanoparticle vaccine protects hamsters against Alpha and Beta virus variant challenge. *NPJ Vaccines* **6**, 129 (2021).

84. R. Martinez David, A. Schäfer, R. Leist Sarah, G. De la Cruz, A. West, N. Atochina-Vasserman Elena, C. Lindesmith Lisa, N. Pardi, R. Parks, M. Barr, D. Li, B. Yount, O. Saunders Kevin, D. Weissman, F. Haynes Barton, A. Montgomery Stephanie, S. Baric Ralph, Chimeric spike mRNA vaccines protect against Sarbecovirus challenge in mice. *Science* **373**, 991–998 (2021).

85. C. F. Houlihan, N. Vora, T. Byrne, D. Lewer, G. Kelly, J. Heaney, S. Gandhi, M. J. Spyer, R. Beale, P. Cherepanov, D. Moore, R. Gilson, S. Gamblin, G. Kassiotis, L. E. McCoy, C. Swanton, A. Hayward, E. Nastouli, Pandemic peak SARS-CoV-2 infection and seroconversion rates in London frontline health-care workers. *Lancet* **396**, e6–e7 (2020).

86. C. T. Deakin, G. H. Cornish, K. W. Ng, N. Faulkner, W. Bolland, J. Hope, A. Rosa, R. Harvey, S. Hussain, C. Earl, B. R. Jebson, M. Wilkinson, L. R. Marshall, K. O'Brien, E. C. Rosser, A. Radziszewska, H. Peckham, H. Patel, J. Heaney, H. Rickman, S. Paraskevopoulou, C. F. Houlihan, M. J. Spyer, S. J. Gamblin, J. McCauley, E. Nastouli, M. Levin, P. Cherepanov, C. Ciurtin, L. R. Wedderburn, G. Kassiotis, Favorable antibody responses to human coronaviruses in children and adolescents with autoimmune rheumatic diseases. *Med (N Y)* **2**, 1093–1109 (2021).

87. F. Saito, K. Hirayasu, T. Satoh, C. W. Wang, J. Lusingu, T. Arimori, K. Shida, N. M. Q. Palacpac, S. Itagaki, S. Iwanaga, E. Takashima, T. Tsuboi, M. Kohyama, T. Suenaga, M. Colonna, J. Takagi, T. Lavstsen, T. Horii, H. Arase, Immune evasion of Plasmodium falciparum by RIFIN via inhibitory receptors. *Nature* **552**, 101–105 (2017).

88. V. M. Corman, O. Landt, M. Kaiser, R. Molenkamp, A. Meijer, D. K. Chu, T. Bleicker, S. Brünink, J. Schneider, M. L. Schmidt, D. G. Mulders, B. L. Haagmans, B. van der Veer, S. van den Brink, L. Wijsman, G. Goderski, J. L. Romette, J. Ellis, M. Zambon, M. Peiris, H. Goossens, C. Reusken, M. P. Koopmans, C. Drosten, Detection of 2019 novel coronavirus (2019-nCoV) by real-time RT-PCR. *Euro Surveill.* **25**, 2000045 (2020).

Data and materials availability: All data associated with this study are present in the paper or the Supplementary Materials. All unique and stable reagents generated in this study are available by contacting G.K. This work is licensed under a Creative Commons Attribution 4.0 International (CC BY 4.0) license, which permits unrestricted use, distribution, and reproduction in any medium, provided that the original work is properly cited. To view a copy of this license, visit http://creativecommons.org/licenses/by/4.0/. This license does not apply to figures/photos/artwork or other content included in the article that is credited to a third party; obtain authorization from the rights holder before using this material.

Ng *et al.*, *Sci. Transl. Med.* **14**, eabn3715 (2022)   27 July 2022

15 of 15

Science Translational Medicine

SARS-CoV-2 S2–targeted vaccination elicits broadly neutralizing antibodies

Kevin W. NgNikhil FaulknerKatja FinsterbuschMary WuRuth HarveySaira HussainMaria GrecoYafei LiuSvend KjaerCharles SwantonSonia GandhiRupert BealeSteve J. GamblinPeter CherepanovJohn McCauleyRodney DanielsMichael HowellHisashi AraseAndreas WackDavid L.V. BauerGeorge Kassiotis

A conserved vaccine target

Because variants of SARS-CoV-2 continue to arise and reduce the protection afforded by vaccination or prior infection, it is becoming increasingly important that vaccines be developed that target more conserved regions of the SARS-CoV-2 spike protein. Here, Ng *et al.* tested whether antibodies targeting the more conserved S2 subunit of the spike protein could confer protection against infection with distinct coronaviruses. The authors observed that S2-targeted vaccination produced antibodies in mice that could neutralize diverse alphacoronaviruses and betacoronaviruses. These antibodies had increased breadth relative to antibodies elicited by full-length spike protein vaccination, suggesting less repertoire focusing. Thus, S2-targeted vaccination may be a strategy to achieve pan-SARS-CoV-2 immunity.

View the article online
https://www.science.org/doi/10.1126/scitranslmed.abn3715
Permissions
https://www.science.org/help/reprints-and-permissions

Use of this article is subject to the Terms of service